Electronic Supplementary Material (ESI) for Journal of Materials Chemistry A.

Electronic Supplementary Information

Fast Water Transport Through Sub-5 nm Polyamide Nanofilms: The New Upper-Bound of the Permeance-Selectivity Trade-Off in Nanofiltration

Pulak Sarkar[a,b], Solagna Modak[a,†], Santanu Ray[c,‡], Vasista Adupa[d], K. Anki Reddy[d], Santanu Karan[a,b,*]

[a]Membrane Science and Separation Technology Division, CSIR-Central Salt and Marine Chemicals Research Institute, G. B. Marg, Bhavnagar, Gujarat 364002, India.

[b]Academy of Scientific and Innovative Research (AcSIR), Ghaziabad, Uttar Pradesh 201002, India.

[c]School of Environment and Technology, University of Brighton, Brighton BN2 4GJ, United Kingdom.

[d]Department of Chemical Engineering, Indian Institute of Technology Guwahati, Assam 781039, India.

Present Addresses: †Hooghly Women's College, Pipulpati, Hooghly, West Bengal 712103, India. ‡Ceres Power Limited, Viking House, Foundry Lane, Horsham RH13 5PX, United Kingdom.

*Corresponding author. E-mail: santanuk@csmcri.res.in

Materials and methods

Chemicals and materials

Polyacrylonitrile (PAN) powder was received from IPCL, India. Piperazine (reagentplus® 99%), trimesoyl chloride (TMC, 98%), and sodium lauryl sulfate (SLS, AR, ≥99%) were purchased from Sigma Aldrich, India. *n*-hexane (99%, HPLC), sodium sulphate (Na_2SO_4, 99.5%), magnesium chloride ($MgCl_2$, 99%), sodium chloride (NaCl, 99.9%), magnesium sulphate ($MgSO_4$, 99%), and methanol (extra pure AR, 99.8%) were purchased from Sisco Research Laboratories Pvt. Ltd. (SRL), India. Isopropanol (extra pure) was purchased from S. D. Fine-Chem Limited, India. Dimethylformamide (DMF, EMPLURA®, 99%) was purchased from MERCK life science Pvt. Ltd., India. Ultrapure water for membrane preparation was produced by Elix® Essential 3 Water Purification System, Merck Life Science Pvt. Ltd., Darmstadt, Germany. N-type <100> silicon wafers were purchased from University wafer, Boston, USA, and used as a substrate for atomic force microscopy (AFM) and scanning electron microscopy (SEM) study. Nonwoven polyester fabric (Nordlys-TS100) was used for making porous support made via phase inversion. PLATYPUS™ (Platypus technologies LLC, USA) silicon wafers with 100 nm thick gold coating were purchased from Agar Scientific, UK, and used for X-ray photoemission spectroscopy (XPS) studies. Flat sheets of commercial nanofiltration membrane (Dow FILMTEC™ NF270) were purchased from Sterlitech, USA. High resolution noncontact "golden" silicon AFM cantilevers (NSG10 series) was obtained from NT-MDT Spectrum Instruments, Moscow, Russia. PointProbe® Plus silicon-SPM probes (PPP-NCH) were obtained from Nanosensors™, Switzerland. RO treated water (conductivity < 200 µS) was used in the gelation bath for making ultrafiltration membranes via phase inversion. Pure water (conductivity < 2 µS) was prepared from a multi-pass RO system and used as a feed to study the nanofiltration performance of the composite membranes. Porous Anodisc™ alumina supports (Whatman™; 0.2 µm) were obtained from Whatman International Ltd., England, and used for cross-sectional SEM study.

Characterization methods

Scanning electron microscope (SEM) study

Polyamide nanofilm fabricated on hydrolyzed polyacrylonitrile (PAN) support was analyzed using a high-resolution scanning electron microscope (SEM, JEOL JSM 7100F, Japan) with an accelerating voltage of 15 kV. The composite membranes were cleaned with methanol and dried in a hot air oven at 50 °C for 10 minutes for imaging. A 2 – 4 nm thick gold was sputtered coated (EM ACE200, Leica Microsystems) to achieve a conducting surface for the SEM imaging.

Atomic force microscope (AFM) study

The surface morphology and thickness of the nanofilms were measured by NT-MDT, NTEGRA Aura Atomic Force Microscopy (AFM) with a pizzo type scanner, and NSG10 series cantilevers. A few samples were also characterized with Bruker Dimension 3100 under tapping mode using PointProbe® Plus silicon-SPM probe. For the thickness measurement of the polyamide nanofilm, nanofilm was detached from its composite structure and transferred onto a silicon wafer (see experimental section), and dried at room temperature. Nanofilm with silicon wafer was cleaned with methanol by immersing in methanol for 15 min and dried in a hot air oven at 50 ºC for 15 minutes. A scratch was made on the nanofilm surface with a sharp scalpel to reveal the wafer surface and allow measurement of the height from the silicon wafer surface to the upper nanofilm surface. The step height (the difference between the height of the wafer surface and the nanofilm surface) is the thickness of the nanofilm. Gwyddion 2.52 SPM data visualization and analysis software was used for image processing.

Measurement of zeta potential

The surface zeta potential of the nanofilms was measured by ZetaCad streaming current & zeta potential meter, CAD Instruments, France. The composite membranes made on HPAN support were wetted in water for several hours and fixed in a dedicated rectangular cell of size 3 cm x 5 cm. The system was washed by running pure water (conductivity < 2 µS) before each test. The steady-state zeta potential was measured with 1 mM KCl electrolyte solution.

X-ray photoelectron spectroscopy (XPS) study

Polymer nanofilms were made freestanding and transferred onto a PLATYPUS™ gold-coated silicon wafer. The gold-coated silicon wafer containing nanofilm was then dried at room temperature, washed in methanol by immersing in methanol for 15 min, and finally dried in a hot air oven at 50 °C for 15 min. The XPS analysis was carried out using a Thermo Scientific ESCALAB 250 Xi photoelectron spectrometer (XPS) using a monochromatic AlKα X-ray as an excitation source outfitted with an X-ray spot size of 650 × 650 μm^2. The survey spectra and core-level XPS spectra were recorded from at least three different spots on the samples. The analyzer was operated at a pass energy of 150 eV for survey scans and 20 eV for narrow scans with the C1s peak set at BE 284.5 eV. A low-energy electron flood gun was used to overcome sample charging. Data processing was performed using Thermo Scientific™ Avantage data system and CasaXps processing software. Peak areas were measured after satellite subtraction and background subtraction, either with a linear background or following the methods of Shirley. (D. A. Shirley, High-resolution X-ray photoemission spectrum of the valence bands of gold, Phys. Rev. B 5, 4709, 1972). The deconvolution of the core-level spectra was done by choosing a Shirley or spline Tougaard background with GL(30) line shape (70% Gaussian, 30% Lorentzian) to determine the chemical species of the nanofilm.

Conductivity measurement

Eutech PC2700 conductivity meter was used to measure the individual salt concentration in the feed (C_f) and permeate solution (C_p) in the range of 10 µS to 50 mS. The salt rejection of the composite membranes was calculated from the ratio between the difference in conductivity of feed and permeate solution to the conductivity of the feed solution.

$$\text{Rejection } (\%) = \frac{Cf\ (\text{feed}) - Cp(\text{permeate})}{Cf\ (\text{feed})} \times 100 \quad \text{.....(i)}$$

Inductively coupled plasma mass spectrometry (ICP-MS) measurement

Perkin Elmer, Optima 2000, inductively coupled plasma mass spectrometry (ICP-MS) was used to detect dissolved ions in the feed and permeate solutions. The instrument was calibrated between

0.3 to 10 ppm, and the concentration of the samples was calculated based on the calibration curve. At least four sets (permeates from four membrane coupons) of experiments were carried out to calculate the mean value of the ion rejection and the standard deviation of the measurements.

Ion chromatography (IC) measurement

The ion chromatography (IC) technique was used to measure the concentrations of anions such as chloride and sulfate. Thermo Scientific™ Dionex™ ICS-5000+ instrument was used to quantify the ions in the feed and permeate samples after dilution. The instrument was calibrated between 0.02 to 50 ppm, and the concentration of the samples was calculated based on the calibration curve. At least four sets (permeates from four membrane coupons) of experiments were carried out to calculate the mean value of the ion rejection and the standard deviation of the measurements.

Membrane fabrication

Preparation of hydrolyzed polyacrylonitrile (HPAN) ultrafiltration support membranes

Polyacrylonitrile (PAN) polymer powder was kept in a hot air oven at 70 °C for two hours. 13.0 wt% solution was prepared by dissolving the polymer in DMF under vigorous stirring at 60 °C for overnight. The dope solution was cast on the nonwoven fabric in a semi-automatic roll-to-roll casting machine by maintaining the gap between the knife and the nonwoven fabric at 150 (±5) µm and allows forming the UF support membrane via phase inversion in the water bath containing RO treated water (TDS: 180 ppm). Typically, a membrane roll of 20 m length and 30 cm wide was cast at a speed of 5 m min^{-1} at a constant temperature of 26 (±1) °C. Finally, the membrane was cut into rectangular pieces (16 cm x 27 cm), washed with pure water (conductivity ~ 2 µS), and stored in isopropanol and water mixture (1:1 v/v) at 10 (±1) °C. For the hydrolysis of PAN ultrafiltration supports, several pieces (~75 nos.) of PAN supports were taken out from the storage solution and washed thoroughly in pure water. Supports were then immersed in a 5 L of 1 M sodium hydroxide (NaOH) solution preheated in a hot air oven at 60 (±1) °C for 2 h, and the solution was reheated in the hot air oven at 60 (±1) °C for 2 h to allow hydrolysis. After hydrolysis, HPAN membranes were

transferred in pure water and repeatedly washed in freshwater. Finally, the HPAN membranes were stored in isopropanol and water mixture (1:1 v/v) at 10 (±1) °C.

Preparation of polyamide nanofilm composite membranes

Sub-5 nm polyamide nanofilms were prepared via the conventional interfacial polymerization method. HPAN support was washed with pure water to remove isopropanol and then soaked for 20 s in an aqueous PIP solution (concentration varying from 0.05 wt% to 3.0 wt%). The aqueous PIP solution was discarded, and the droplets that remained on the support surface were removed with a rubber roller and further air-dried for 10 – 30 s to remove any excess water from the top surface. The support, in this case, will remain moist, not dried. Instantly, the hexane solution containing TMC (concentration varying from 0.05 wt% to 0.15 wt%) was poured on the top of PIP soaked HPAN support and reacted for 5 – 60 s to happen interfacial polymerization reaction (Table S1†). TMC solution was then discarded, and the surface of the nascent nanofilm formed on the support was washed with hexane by pouring pure hexane on the surface (post-solvent-washing) to remove unreacted TMC molecules. Hexane was then discarded, and the composite membrane was post-heated in a hot air oven at a designated temperature and time. The post-solvent-washing and post-heating process is named with the acronym PWPH. To establish the transferability and widespread applicability of the post-solvent-washing treatment, nanofilm composite membranes were prepared in the presence of sodium lauryl sulfate (SLS) added with PIP in the aqueous phase,[1] and similar post-solvent-washing and post-heating was adopted as explained above. In some cases, repeated post-solvent-washing with multiple solvents were conducted to realize the solvent stability of the sub-5 nm nanofilm. In addition to the post-solvent-washing and post-heating (PWPH), nanofilm composite membranes were also prepared with (i) post-washing and no post-heating; PWNH, (ii) no post-washing and only post-heating; NWPH, and (iii) post-heating and then post-washing; PHPW.

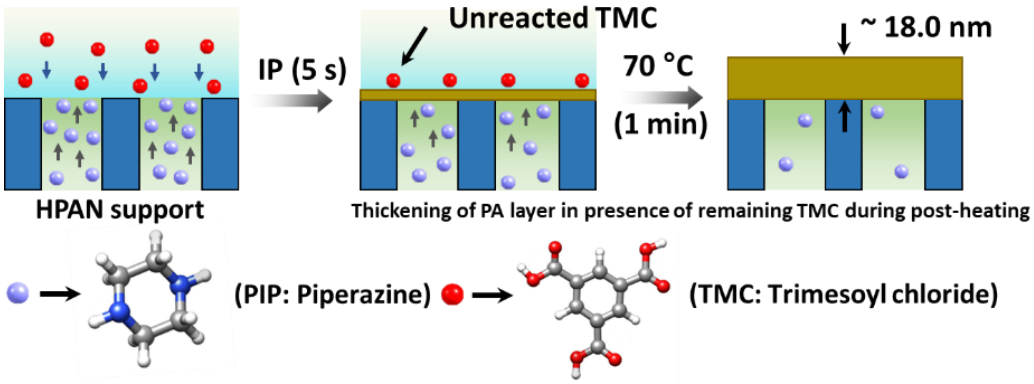

Figure S1: Schematic presentation of the preparation process of nanofilm composite membranes via conventional interfacial polymerization technique followed without any post solvent rinsing/washing method.

Fabrication of freestanding nanofilm from the composite membrane and transferred onto different substrates (the front surface of the freestanding nanofilm is on the top)

Nanofilm composite membranes, as listed in Table S1, were prepared on top of polyacrylonitrile support. The membrane was immersed in acetone for 30 min, and the fabric was peeled off. PAN support with the nanofilm on top was floated on DMF containing 2 v/v% water and left overnight to dissolve PAN from the rear side of the polyamide nanofilm.[1] The isolated nanofilm was then transferred on different substrates (silicon wafer, porous alumina, gold-coated silicon wafer) facing the front surface on the top. The nanofilm with the substrate was then dried in a hot air oven at 50 (±1) °C for 15 min to improve adhesion with the support. The nanofilm was washed with DMF by immersing in DMF overnight and dried at 50 (±1) °C for 15 min in a hot air oven and further washed in methanol by immersing in methanol for 15 min and finally dried at 50 (±1) °C in a hot air oven for 15 min before characterization.[1]

Table S1: Preparation conditions of polyamide nanofilms via interfacial polymerization on PAN or HPAN support using PIP in the aqueous phase and TMC in the hexane phase.

Polyamide nanofilm (amine wt%-TMC wt%-post-treatment)	Aqueous amine phase [wt%] + SLS [mM]	TMC in organic phase [wt%]	IP time [s]	Post-treatment of the nascent nanofilm	
				Step 1	Step 2
NFM #1: PIP-0.05%-0.1%-PWPH	PIP [0.05]	TMC [0.1]	5	Washing with hexane	70 °C for 1 min
NFM #2: PIP-0.1%-0.1%-PWPH	PIP [0.1]	TMC [0.1]	5	Washing with hexane	70 °C for 1 min
NFM #3: PIP-1.0%-0.1% -PWPH	PIP [1.0]	TMC [0.1]	5	Washing with hexane	70 °C for 1 min
NFM #4: PIP-2.0%-0.05%-PWPH	PIP [2.0]	TMC [0.05]	5	Washing with hexane	70 °C for 1 min
NFM #5: PIP-2.0%-0.1%-PWPH	PIP [2.0]	TMC [0.1]	5	Washing with hexane	70 °C for 1 min
NFM #6: PIP-2.0%-0.15%-PWPH	PIP [2.0]	TMC [0.15]	5	Washing with hexane	70 °C for 1 min
NFM #7: PIP-0.1%-0.1%-NWNH	PIP [0.1]	TMC [0.1]	5	No washing	No heating
NFM #8: PIP-0.1%-0.1%-PWNH	PIP [0.1]	TMC [0.1]	5	Washing with hexane	No heating
NFM #9: PIP-0.1%-0.1%-PHPW	PIP [0.1]	TMC [0.1]	5	Heating at 70 °C for 1 min	Washing with hexane
NFM #10: PIP-0.05%-0.1%-NWNH	PIP [0.05]	TMC [0.1]	5	No washing	No heating
NFM #11: PIP-0.05%-0.1%-PWNH	PIP [0.05]	TMC [0.1]	5	Washing with hexane	No heating
NFM #12: PIP-2.0%-0.1%-NWNH	PIP [2.0]	TMC [0.1]	5	No washing	No heating
NFM #13: PIP-2.0%-0.1%-PWNH	PIP [2.0]	TMC [0.1]	5	Washing with hexane	No heating
NFM #14: PIP-2.0%-0.1%-NWPH	PIP [2.0]	TMC [0.1]	5	No washing	70 °C for 1 min
NFM #15: PIP-2.0%-0.1%-NWPH[a]	PIP [2.0]	TMC [0.1]	5	No washing	80 °C for 1 min
NFM #16: PIP-2.0%-0.1%-PWPH[a]	PIP [2.0]	TMC [0.1]	5	Washing with hexane	80 °C for 1 min
NFM #17: PIP-3.0%-0.1%-PWPH	PIP [3.0]	TMC [0.1]	5	Washing with hexane	70 °C for 1 min
NFM #18: PIP-0.1%-0.1%-NWPH	PIP [0.1]	TMC [0.1]	5	No washing	70 °C for 1 min
NFM #19: PIP-1.0%-0.1% -NWPH	PIP [1.0]	TMC [0.1]	5	No washing	70 °C for 1 min
NFM #20: PIP-0.05%-0.1%-PWPH[b]	PIP [0.05]	TMC [0.1]	60	Washing with hexane	70 °C for 1 min
NFM #21: PIP-0.05%-0.15%-PWPH	PIP [0.05]	TMC [0.15]	5	Washing with hexane	70 °C for 1 min
NFM #22: PIP-0.1%-0.15%-PWPH	PIP [0.1]	TMC [0.15]	5	Washing with hexane	70 °C for 1 min
NFM #23: PIP-1.0%-0.15%-PWPH	PIP [1.0]	TMC [0.15]	5	Washing with hexane	70 °C for 1 min
NFM #24: PIP-1.0%-0.15%-PWPH[b]	PIP [1.0]	TMC [0.15]	60	Washing with hexane	70 °C for 1 min
NFM #25: PIP-0.05%-0.1%-NWPH	PIP [0.05]	TMC [0.1]	5	No washing	70 °C for 1 min
NFM #26: PIP-0.05%-0.05%-NWPH[c]	PIP [0.05]	TMC [0.05]	5	No washing	70 °C for 1 min
NFM #27: PIP-0.05%+1 mM SLS-0.1%-NWPH[c]	PIP [0.05] + SLS [1 mM]	TMC [0.1]	5	No washing	70 °C for 1 min
NFM #28: PIP-0.05%+1 mM SLS-0.1%-PWPH	PIP [0.05] + SLS [1 mM]	TMC [0.1]	5	Washing with hexane	70 °C for 1 min
NFM #29: PIP-0.1%+1 mM SLS-0.1%-NWPH[c]	PIP [0.1] + SLS [1 mM]	TMC [0.1]	5	No washing	70 °C for 1 min
NFM #30: PIP-0.1%+1 mM SLS-0.1%-PWPH	PIP [0.1] + SLS [1 mM]	TMC [0.1]	5	Washing with hexane	70 °C for 1 min

PIP: piperazine; TMC: trimesoyl chloride; HPAN: hydrolyzed polyacrylonitrile (PAN). PWPH: post-solvent-washing with hexane followed by post-heating at 70 °C for 1 min. NWNH: No solvent-washing and no post-heating. PWNH: post-solvent-washing with hexane and no post-heating. PHPW: post-heating at 70 °C for 1 min followed by post-solvent-washing with hexane. NWPH: no post-solvent-washing and only post-heating at 70 °C for 1 min. [a]Post-heating was done at 80 °C for 5 min. [b]Interfacial polymerization reaction time was 60 s. [c]Data were taken from ref. 1.

Characterization of the nanofilm composite membranes

Nanofilms prepared on HPAN support and characterized by SEM

The surface morphology of the nanofilm composite membranes observed under SEM is presented in Figures S2 and S3.

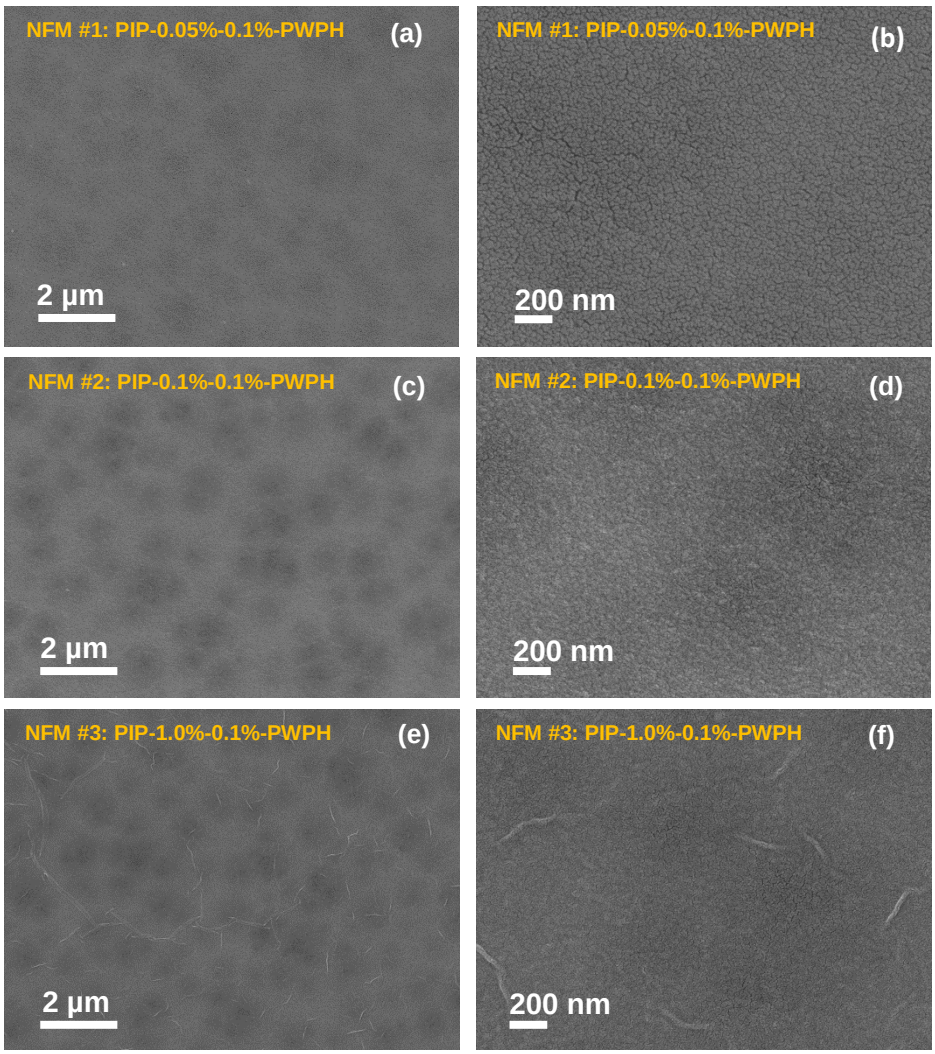

Figure S2: Surface morphology of the nanofilm composite membranes prepared on HPAN support observed under SEM. (a, b) for NFM #1: PIP-0.05%-0.1%-PWPH. (c, d) for NFM #2: PIP-0.1%-0.1%-PWPH. (e, f) for NFM #3: PIP-1.0%-0.1%-PWPH. Images on the right panel are under higher magnification. PWPH: post-solvent-washing with hexane followed by post-heating at 70 °C for 1 min.

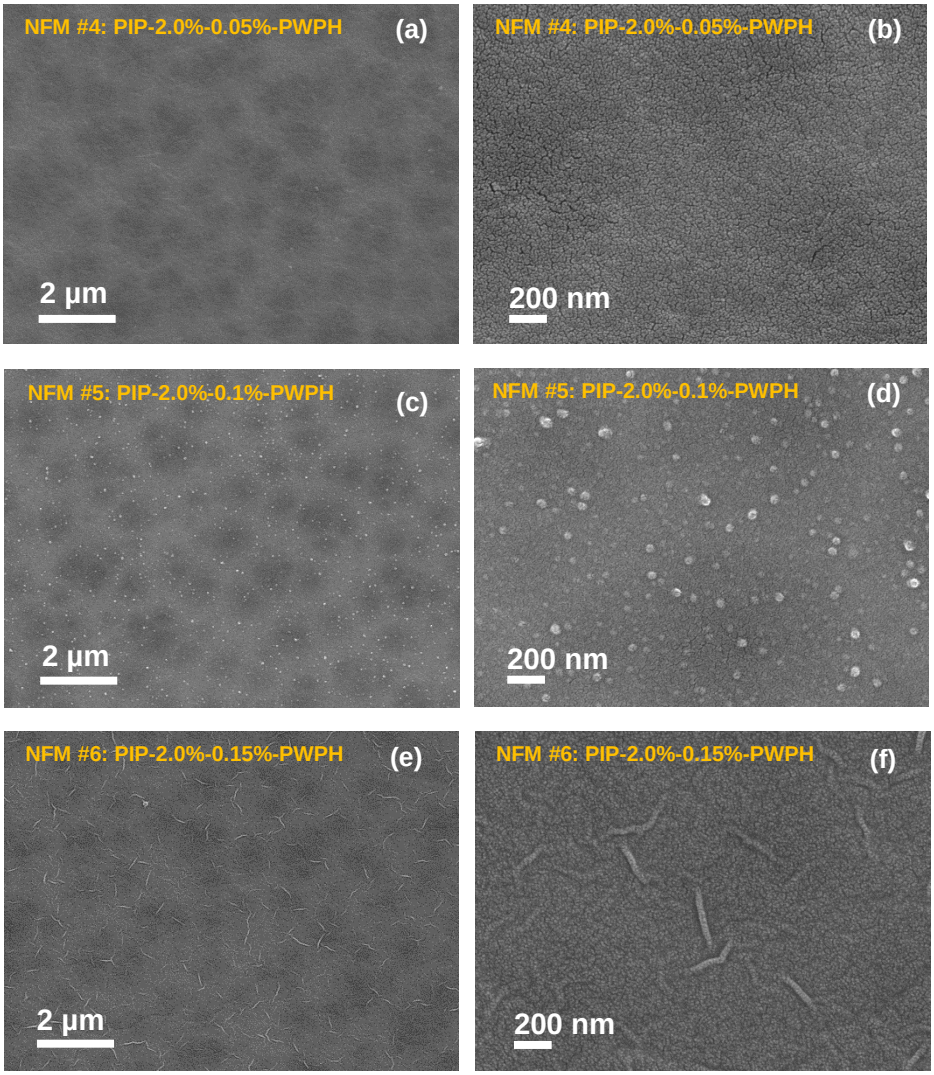

Figure S3: Surface morphology of the nanofilm composite membranes prepared on HPAN support observed under SEM. (a, b) for NFM #4: PIP-2.0%-0.05%-PWPH. (c, d) for NFM #5: PIP-2.0%-0.1%-PWPH. (e, f) for NFM #6: PIP-2.0%-0.15%-PWPH. Images on the right panel are under higher magnification. PWPH: post-solvent-washing with hexane followed by post-heating at 70 °C for 1 min.

Characterization of the freestanding nanofilms by TEM

The freestanding nanofilm prepared from the composite membrane made from 1 wt% PIP and 0.1 wt% TMC and reacted for 5 s on PAN support showed a defect-free and uniform nanofilm over the entire surface of the TEM grid. The TEM image in Figure S4 represents the nanofilm prepared without any post-solvent-washing treatment after interfacial polymerization. The TEM image in Figure S5 represents the PIP nanofilm prepared with post-solvent-washing with hexane after interfacial polymerization.

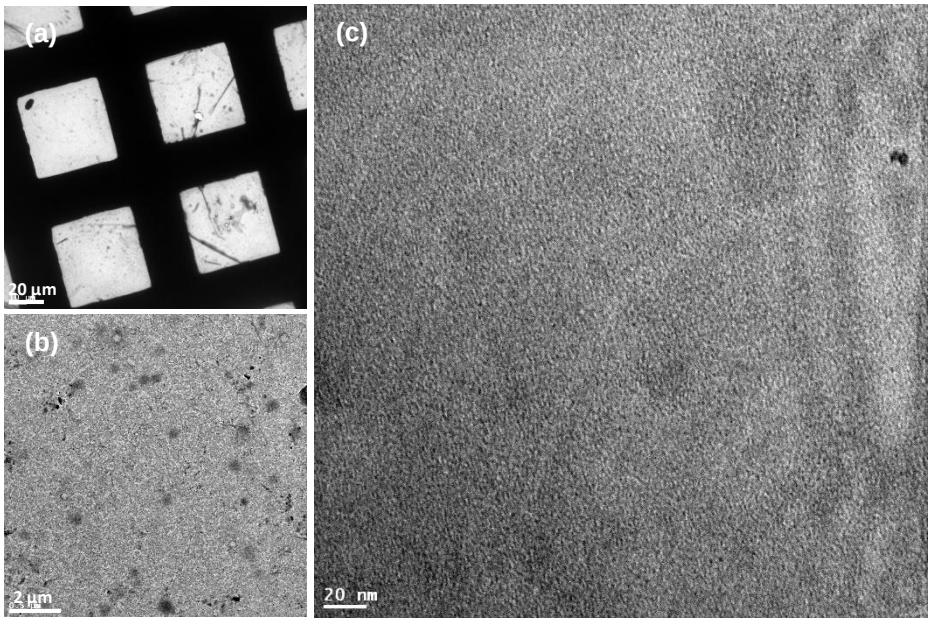

Figure S4: TEM micrograph of the freestanding nanofilm NFM #19 (PIP-1.0%-0.1%-NWPH). NWPH: no post-solvent-washing with hexane but post-heated at 70 °C for 1 min.

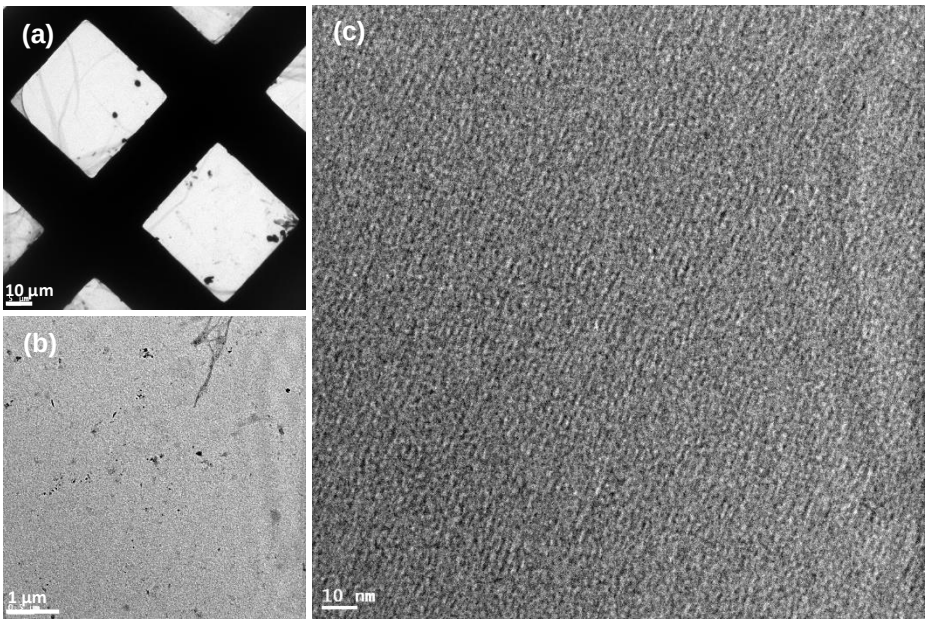

Figure S5: TEM micrograph of the freestanding nanofilm NFM #3 (PIP-1.0%-0.1%-PWPH). PWPH: post-solvent-washing with hexane followed by post-heating at 70 °C for 1 min.

Freestanding nanofilms transferred on to silicon wafer: characterization by AFM

AFM images and height profiles were measured to know the thickness of the nanofilms. Images are presented in Figures S6 – S13.

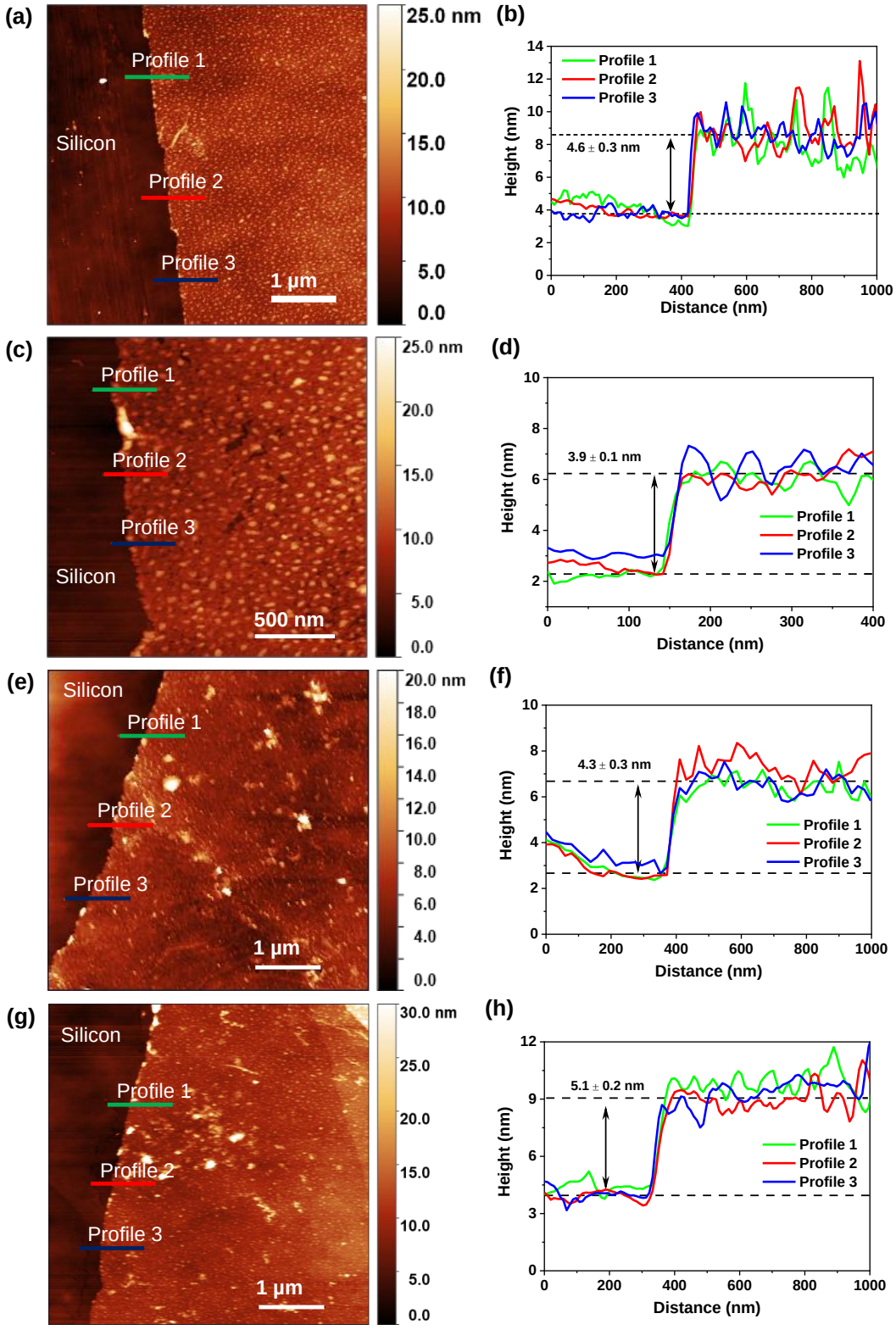

Average thickness from all batches: 4.5 ± 0.5 nm

Figure S6: AFM height images and corresponding height profiles of the polyamide nanofilm (NFM #1: PIP-0.05%-0.1%-PWPH) conducted for different batches. (a, b) batch 1, (c, d) batch 2, (e, f) batch 3, and (g, h) batch 4. PWPH**:** post-solvent-washing with hexane followed by post-heating at 70 °C for 1 min.

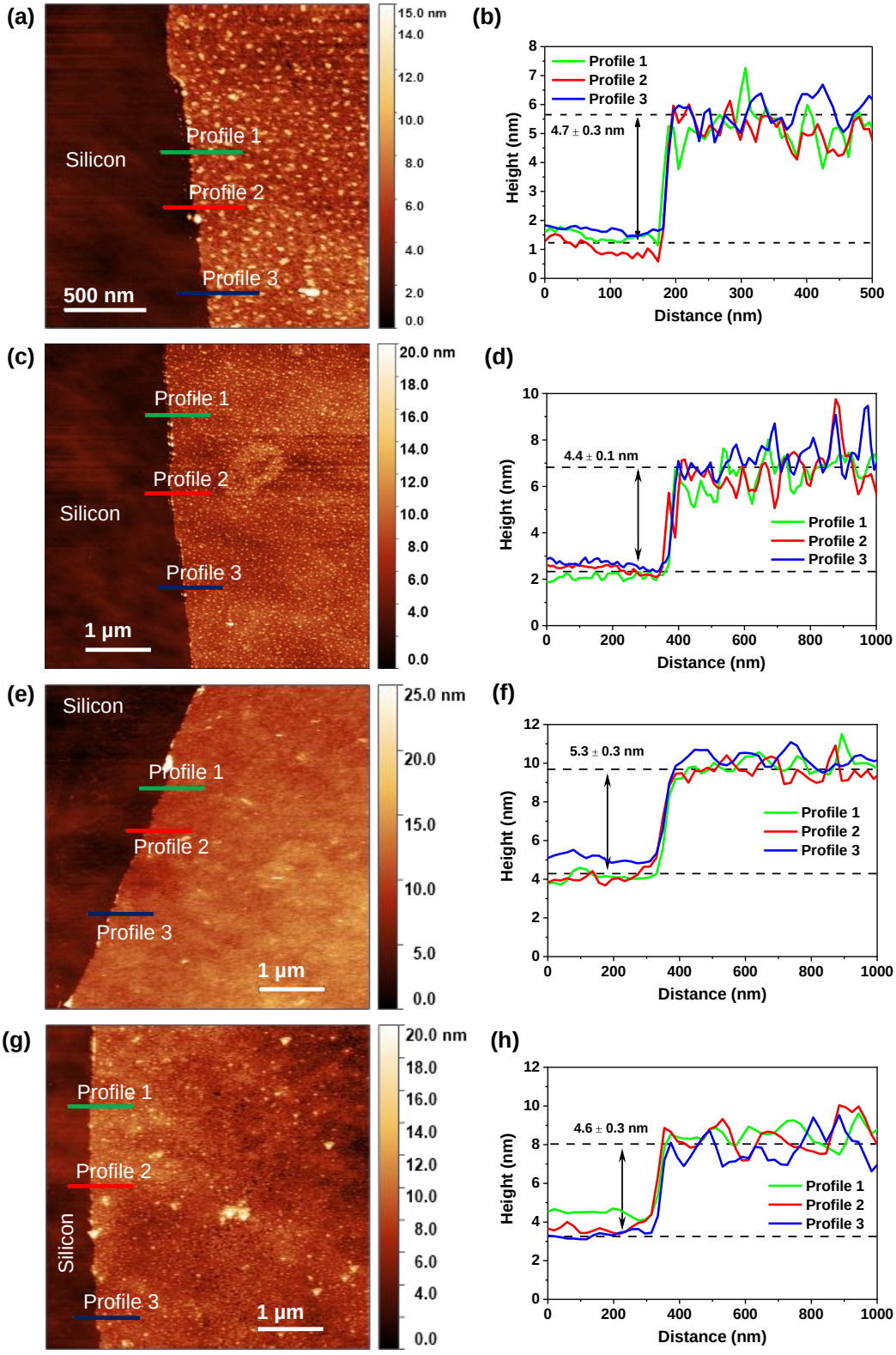

Average thickness from all batches: 4.7 ± 0.4 nm

Figure S7: AFM height images and corresponding height profiles of the polyamide nanofilm (NFM #2: PIP-0.1%-0.1%-PWPH) conducted for different batches. (a, b) batch 1, (c, d) batch 2, (e, f) batch 3, and (g, h) batch 4. PWPH**:** post-solvent-washing with hexane followed by post-heating at 70 °C for 1 min.

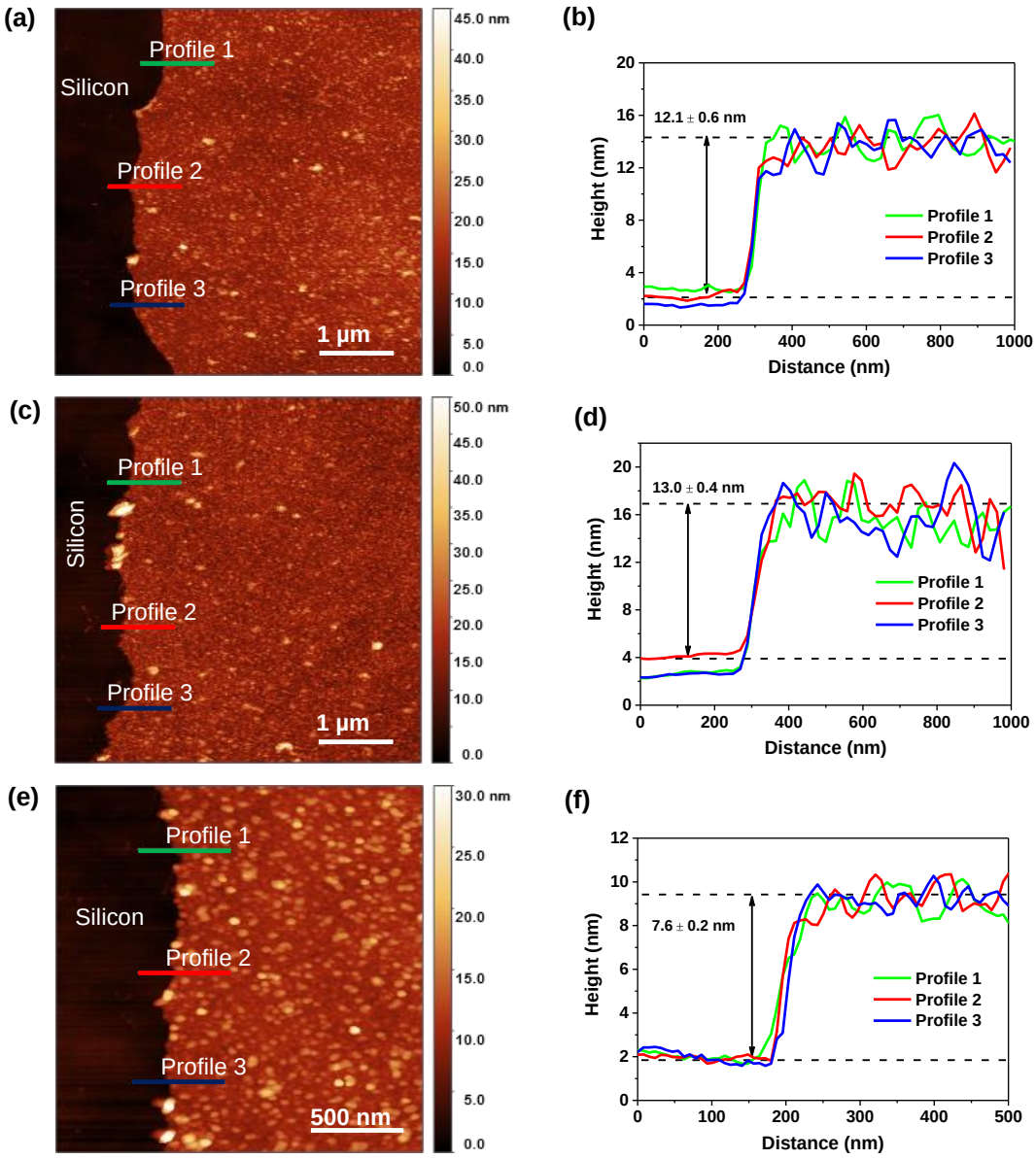

Figure S8: AFM height images and corresponding height profiles of the polyamide nanofilms. (a, b) For the nanofilm NFM #4 (PIP-2.0%-0.05%-PWPH). (c, d) For the nanofilm NFM #5 (PIP-2.0%-0.1%-PWPH). (e, f) For the nanofilm NFM #6 (PIP-2.0%-0.15%-PWPH). PWPH**:** post-solvent-washing with hexane followed by post-heating at 70 °C for 1 min.

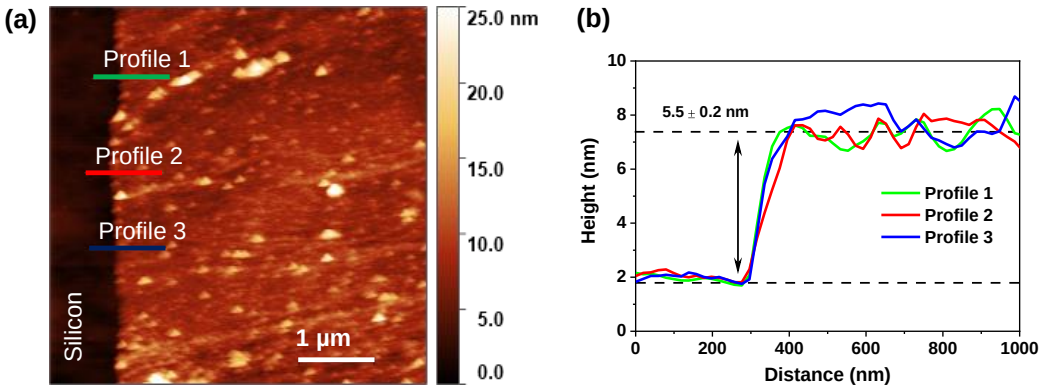

Figure S9: AFM height image and corresponding height profile of the polyamide nanofilm (NFM #8: PIP-0.1%-0.1%-PWNH). PWNH**:** post-solvent-washing with hexane but no post-heating.

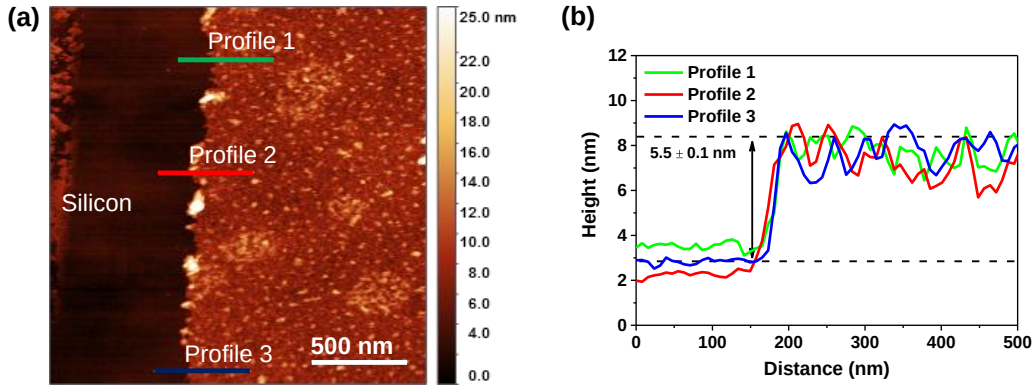

Figure S10: AFM height image and corresponding height profile of the polyamide nanofilm NFM #3 (PIP-1.0%-0.1%-PWPH). PWPH**:** post-solvent-washing with hexane followed by post-heating at 70 °C for 1 min.

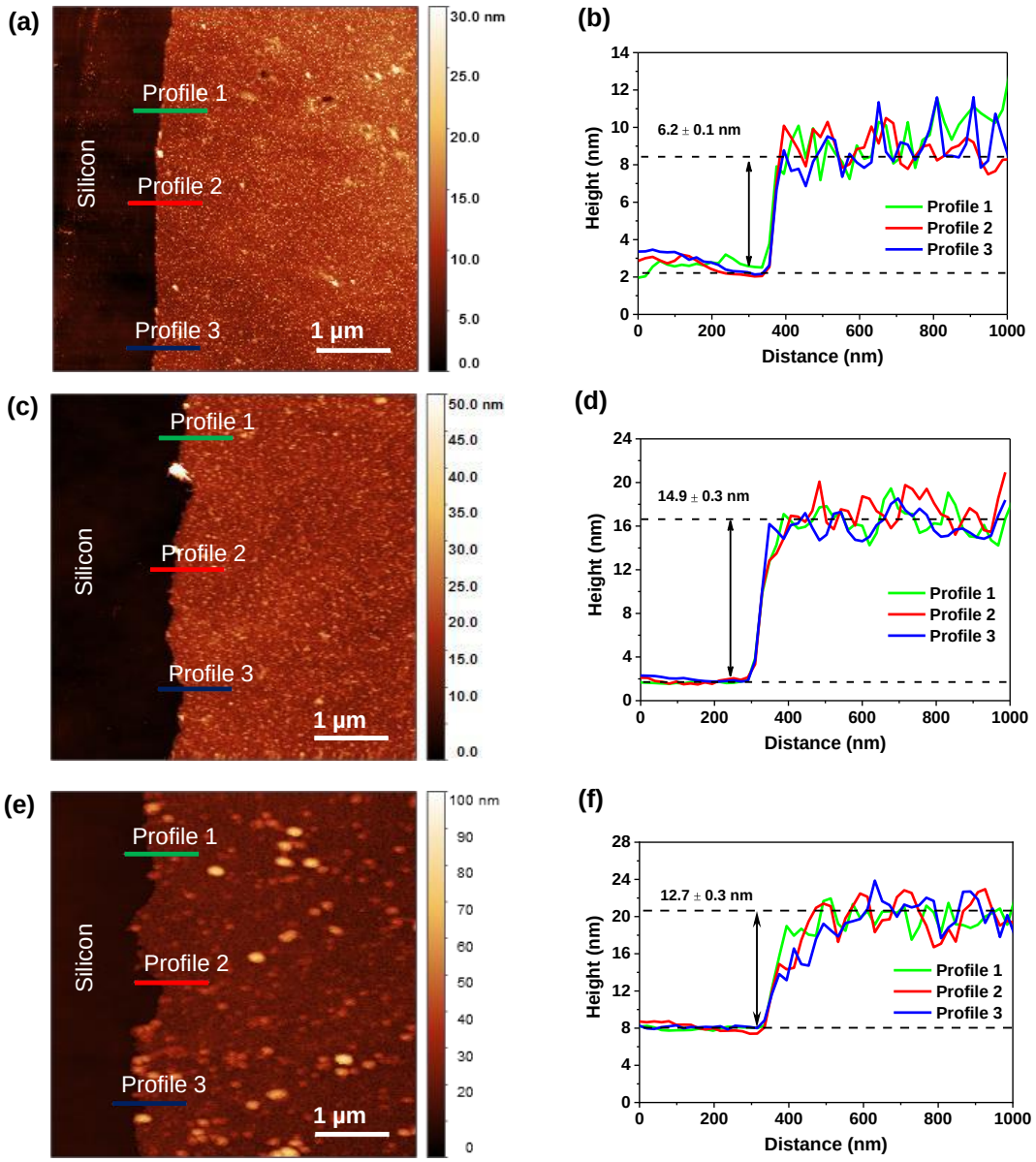

Figure S11: AFM height images and corresponding height profiles of the polyamide nanofilms. (a, b) For the nanofilm NFM #11 (PIP-0.05%-0.1%-PWNH). (c, d) For the nanofilm NFM #15 (PIP-2.0%-0.1%-NWPH[a]). (e, f) For the nanofilm NFM #12 (PIP-2.0%-0.1%-NWNH). PWNH**:** post-solvent-washing with hexane and no post-heating. NWPH[a]**:** post-heating was done at 80 °C for 5 min. NWNH**:** no post-solvent-washing and no post-heating.

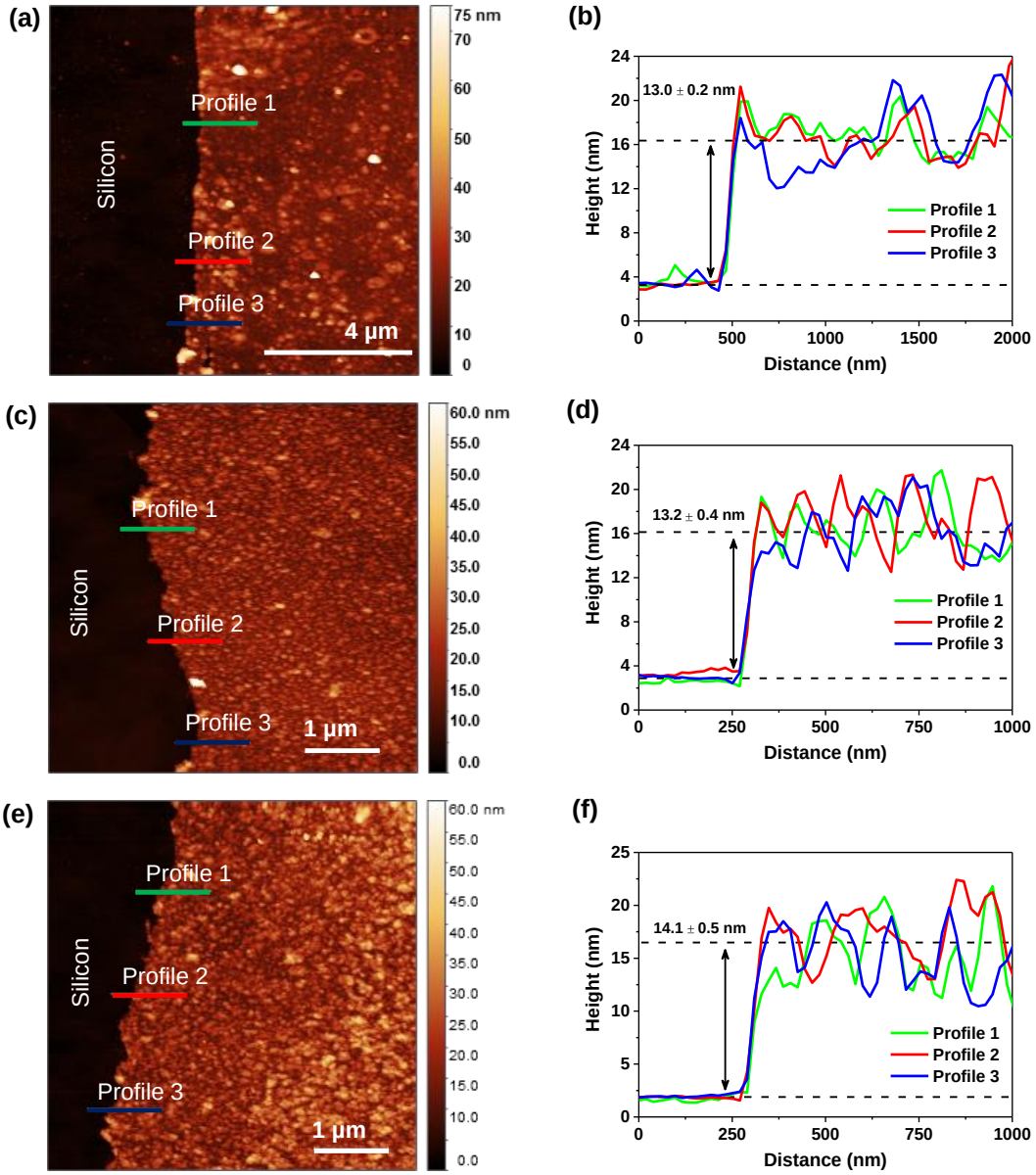

Figure S12: AFM height images and corresponding height profiles of the polyamide nanofilms. (a, b) For the nanofilm NFM #10 (PIP-0.05%-0.1%-NWNH). (c, d) For the nanofilm NFM #13 (PIP-2.0%-0.1%-PWNH). (e, f) For the nanofilm NFM #16 (PIP-2.0%-0.15%-PWPH[a]). NWNH**:** no post-solvent-washing and no post-heating. PWNH**:** post-solvent-washing with hexane and no post-heating. PWPH[a]**:** Post-heating was done at 80 °C for 5 min.

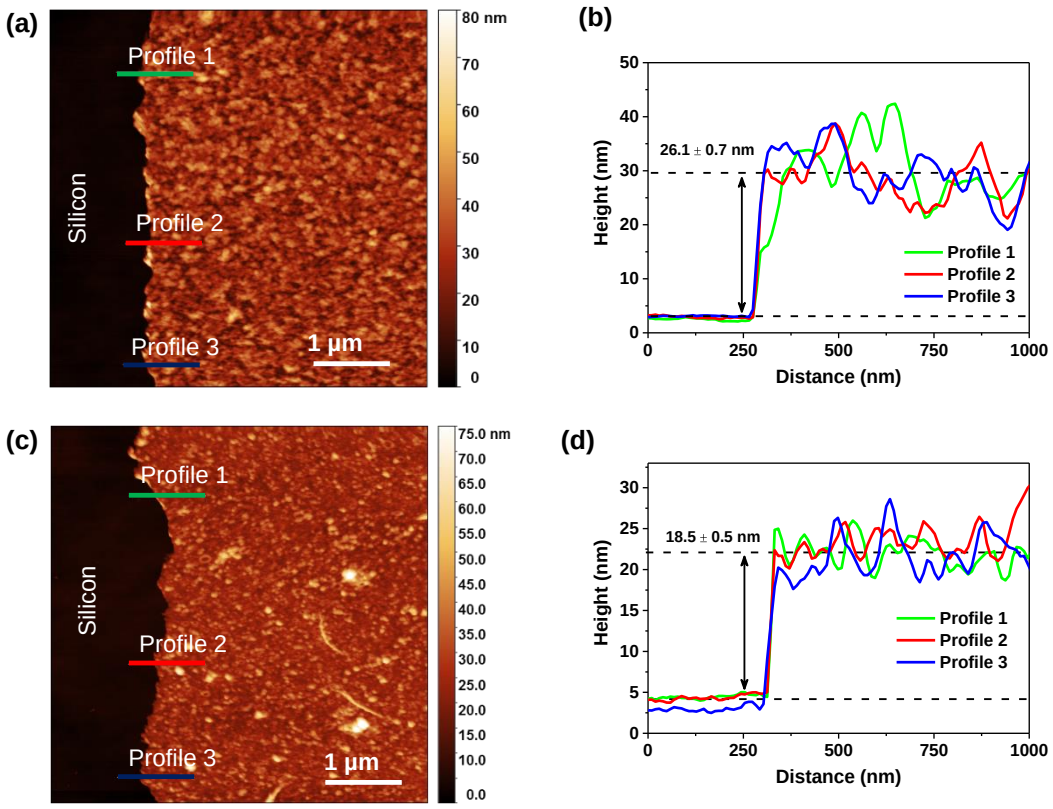

Figure S13: AFM height images and corresponding height profiles of the polyamide nanofilms. (a, b) For the nanofilm NFM #17 (PIP-3.0%-0.1%-PWPH). (c, d) For the nanofilm NFM #14 (PIP-2.0%-0.1%-NWPH). PWPH**:** Post-solvent-washing with hexane followed by post-heating at 70 °C for 1 min. NWPH**:** No solvent-washing and only post-heating at 70 °C for 1 min.

Table S2: Thickness of the polyamide nanofilms measured from AFM and XPS.

Polyamide nanofilm (amine wt%-TMC wt%-post-treatment)	Thickness measured from AFM (nm)	Thickness measured from XPS	Average thickness from AFM and XPS
NFM #1: PIP-0.05%-0.1%-PWPH	4.5 ± 0.5	6.7	5.6 ± 1.5
NFM #2: PIP-0.1%-0.1%-PWPH	4.7 ± 0.4	3.4	4.1 ± 0.9
NFM #3: PIP-1.0%-0.1%-PWPH	5.5 ± 0.1	6.4	5.9 ± 0.6
NFM #4: PIP-2.0%-0.05%-PWPH	12.1 ± 0.6	---	---
NFM #5: PIP-2.0%-0.1%-PWPH	13.0 ± 0.4	12.4	12.7 ± 0.4
NFM #6: PIP-2.0%-0.15%-PWPH	7.6 ± 0.2	---	---
NFM #7: PIP-0.1%-0.1%-NWNH	---	14.3 ± 1.5	---
NFM #8: PIP-0.1%-0.1%-PWNH	5.5 ± 0.2	3.5 ± 0.3	4.5 ± 1.4
NFM #9: PIP-0.1%-0.1%-PHPW	---	5.7 ± 0.3	---
NFM #10: PIP-0.05%-0.1%-NWNH	13.0 ± 0.2	---	---
NFM #11: PIP-0.05%-0.1%-PWNH	6.2 ± 0.1	---	---
NFM #12: PIP-2.0%-0.1%-NWNH	12.7 ± 0.3	---	---
NFM #13: PIP-2.0%-0.1%-PWNH	13.2 ± 0.4	---	---
NFM #14: PIP-2.0%-0.1%-NWPH	18.5 ± 0.5	---	---
NFM #15: PIP-2.0%-0.1%-NWPH[a]	14.9 ± 0.3	---	---
NFM #16: PIP-2.0%-0.1%-PWPH[a]	14.1 ± 0.5	---	---
NFM #17: PIP-3.0%-0.1%-PWPH	26.1 ± 0.7	---	---
NFM #18: PIP-0.1%-0.1%-NWPH	18.0 ± 0.3[#]	---	---
NFM #25: PIP-0.05%-0.1%-NWPH	11.8 ± 0.2[#]	---	---
NFM #26: PIP-0.05%-0.05%-NWPH	7.3 ± 0.7[#]	---	---

PWPH: post-solvent-washing with hexane followed by post-heating at 70 °C for 1 min. NWNH: no post-solvent-washing and no post-heating. PWNH: post-solvent-washing with hexane and no post-heating. PHPW: post-heating at 70 °C for 1 min followed by post-solvent-washing with hexane. NWPH: no post-solvent-washing and only post-heating at 70 °C for 1 min. [a]Post-heating was done at 80 °C for 5 min. [#]Data were taken from ref. 1.

Molecular dynamics simulation study of the polyamide nanofilm

A molecular dynamics study was carried out to understand the structure of the nanofilm at the molecular level. All the simulations were performed using NAMD[35] software package, and the forcefield used is CHARMM36.[36,37] For the present study, the polyamide nanofilm was prepared by a heuristic approach where crosslinking of the monomers was based on the distance criteria. Initially, TMO (hydrolyzed TMC) and piperazine monomers were placed randomly in a computational box using Packmol [J. Comput. Chem. 2009, 30, 2157–2164]. Minimization was done for 10000 steps, and the system was allowed to equilibrate for 2 ns in NPT ensemble at a temperature of 300 K and 1 atm pressure. After this, the system was subjected to an annealing

process, where the temperature was raised from 300 K to 1100 K at a regular interval and subsequent cooling to 300 K with a step of 50 K in an NVT ensemble. The simulation was continued by allowing new amide bond formation for every 10 ps of simulation time. Initially, the bond formation was allowed only when the distance between C1/C2/C3 of TMO and N1/N2 of piperazine (Figure S14) was less than 2.5 Å. As the simulation progressed, this was relaxed to 3.5 Å with a step of 0.1 Å to speed up the crosslinking process. Energy minimization and equilibration were performed after each crosslinking step. In the end, the unreacted monomers were removed from the nanofilm. The resulting polymer structure was minimized for 10000 steps and equilibrated for 2 ns in the NPT ensemble. After equilibration, the final polymer nanofilm structure was 43 Å thick and 120 Å x 120 Å in the X and Y direction. In the nanofilm after polymerization, the number of reacted sites in TMO were 1274, and the unreacted sites were 1480. In piperazine, the number of reacted sites were 1274, and unreacted sites were 792.

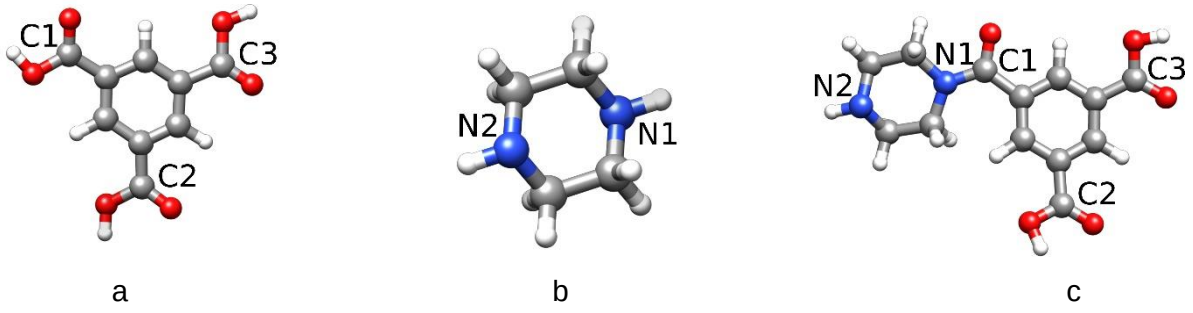

Figure S14: Monomers used in the simulation work: (a) TMO, (b) Piperazine, and (c) Formation of an amide bond between N1 of piperazine & C1 of TMO.

Chemical characterization

Type of chemical structures formed via interfacial polymerization

There will be a probability of having both network crosslinking and linear crosslinking structures in the polyamide made via interfacial polymerization.[1] The chemical structure of fully aromatic polyamide and linearly crosslinked part formed via interfacial polymerization is shown in Figure S15.

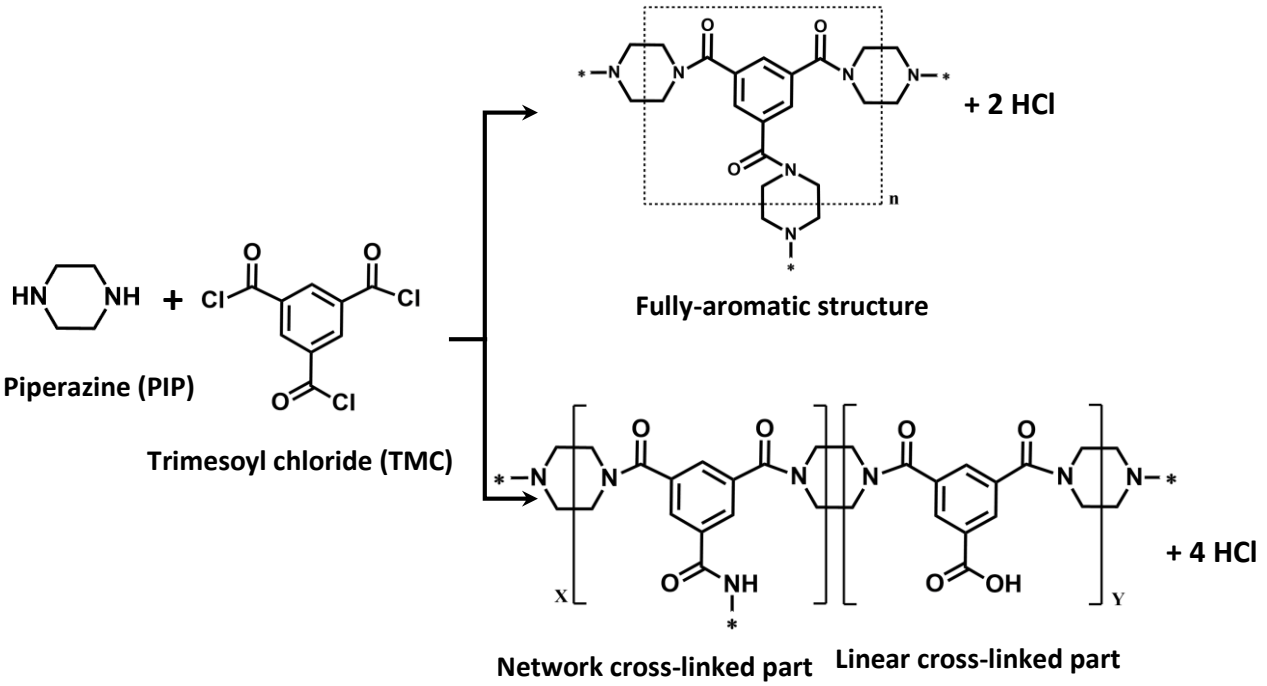

Figure S15: Chemical structures of (a) fully crosslinked and (b) fully linear polyamide prepared from the interfacial polymerization of piperazine (PIP) and trimesoyl chloride (TMC). The unit of the repeated pattern is presented in the dotted box.

Chemical characterization of the freestanding polyamide nanofilms using XPS

The elemental composition of the freestanding polyamide nanofilms was determined from XPS results. The percentage of the elements present are carbon (C), nitrogen (N), and oxygen (O) which are determined from C1s, O1s, and N1s core level XPS spectra. The results from the survey spectra, C1s, O1s, and N1s core level XPS spectra are presented in Tables S3 – S4 and Figures S16 – S19.

The degree of network crosslinking (DNC) of the polyamide nanofilms was measured from the following equation (S2).[1]

$$\mathbf{DNC} = \frac{\mathbf{X}}{\mathbf{X+Y}} \times \mathbf{100}\ \% \qquad \text{..... (S2)}$$

$$\text{where } \frac{\mathbf{O}}{\mathbf{N}} = \frac{\mathbf{3X+4Y}}{\mathbf{3X+2Y}} \qquad \text{..... (S3)}$$

Table S3: XPS results of the freestanding polyamide nanofilms.

Polyamide nanofilm (amine wt%-TMC wt%-post-treatment)	C (at %)	N (at %)	O (at %)	O/N	DNC[1,7] (%)	$\frac{C-N}{(N-C=O/O-C=O)}$ [1] See table S4 and ref. [1]	COOH from O1s [overall COOH in the nanofilm] (at%)
NFM #1: PIP-0.05%-0.1%-PWPH	67.6 ± 2.1	11.3 ± 1.0	21.1 ± 2.2	1.87 ± 0.3	9.1	1.8 ± 0.1	8.3 ± 1.1 [1.75]
NFM #2: PIP-0.1%-0.1%-PWPH	72.1 ± 0.7	12.3 ± 1.1	15.5 ± 0.2	1.26 ± 0.1	65.5	1.8 ± 0.05	8.4 ± 0.6 [1.30]
NFM #3: PIP-1.0%-0.1%-PWPH	72.4 ± 0.7	14.4 ± 0.8	13.2 ± 0.2	0.92 ± 0.1	---	2.2 ± 0.2	4.8 ± 0.1 [0.63]
NFM #5: PIP-2.0%-0.1%-PWPH	71.3 ± 0.4	14.8 ± 0.4	13.9 ± 0.1	0.94 ± 0.03	---	1.6 ± 0.01	4.5 ± 0.4 [0.63]
NFM #7: PIP-0.1%-0.1%-NWNH	68.2 ± 1.7	11.7 ± 0.8	20.1 ± 1.8	1.72 ± 0.2	20.6	1.5 ± 0.2	9.2 ± 0.3 [1.85]
NFM #8: PIP-0.1%-0.1%-PWNH	72.9 ± 0.5	12.7 ± 0.6	14.4 ± 0.9	1.13 ± 0.1	81.7	2.2 ± 0.05	3.4 ± 0.1 [0.49]
NFM #9: PIP-0.1%-0.1%-PHPW	69.1 ± 2.0	12.1 ± 1.0	18.8 ± 1.0	1.56 ± 0.05	34.4	1.8 ± 0.1	11.2 ± 1.8 [2.10]
NFM #18: PIP-0.1%-0.1%-NWPH	74.2 ± 0.3	9.2 ± 0.2	16.6 ± 0.4	1.8 ± 0.1	14.3	1.5 ± 0.1	6.9 ± 1.7 [1.15]

PWPH: post-solvent-washing with hexane and post-heating at 70 °C for 1 min. NWNH: no post-solvent-washing and no post-heating. PWNH: post-solvent-washing with hexane and no post-heating. PHPW: post-heating at 70 °C for 1 min and post-solvent-washing with hexane. NWPH: no post-solvent-washing and only post-heating at 70 °C for 1 min. The species N-C=O…H and O-C=O…H in O1s are the amides and carboxylic acid groups of polyamide, which are hydrogen-bonded to water or intramolecular hydrogen-bonded between amide and carboxylic acid groups, or intramolecular hydrogen-bonded between carboxylic acid groups. Overall COOH (at%) in the nanofilm = [COOH (at%) from O1s] x [O (at%) from the survey spectrum].

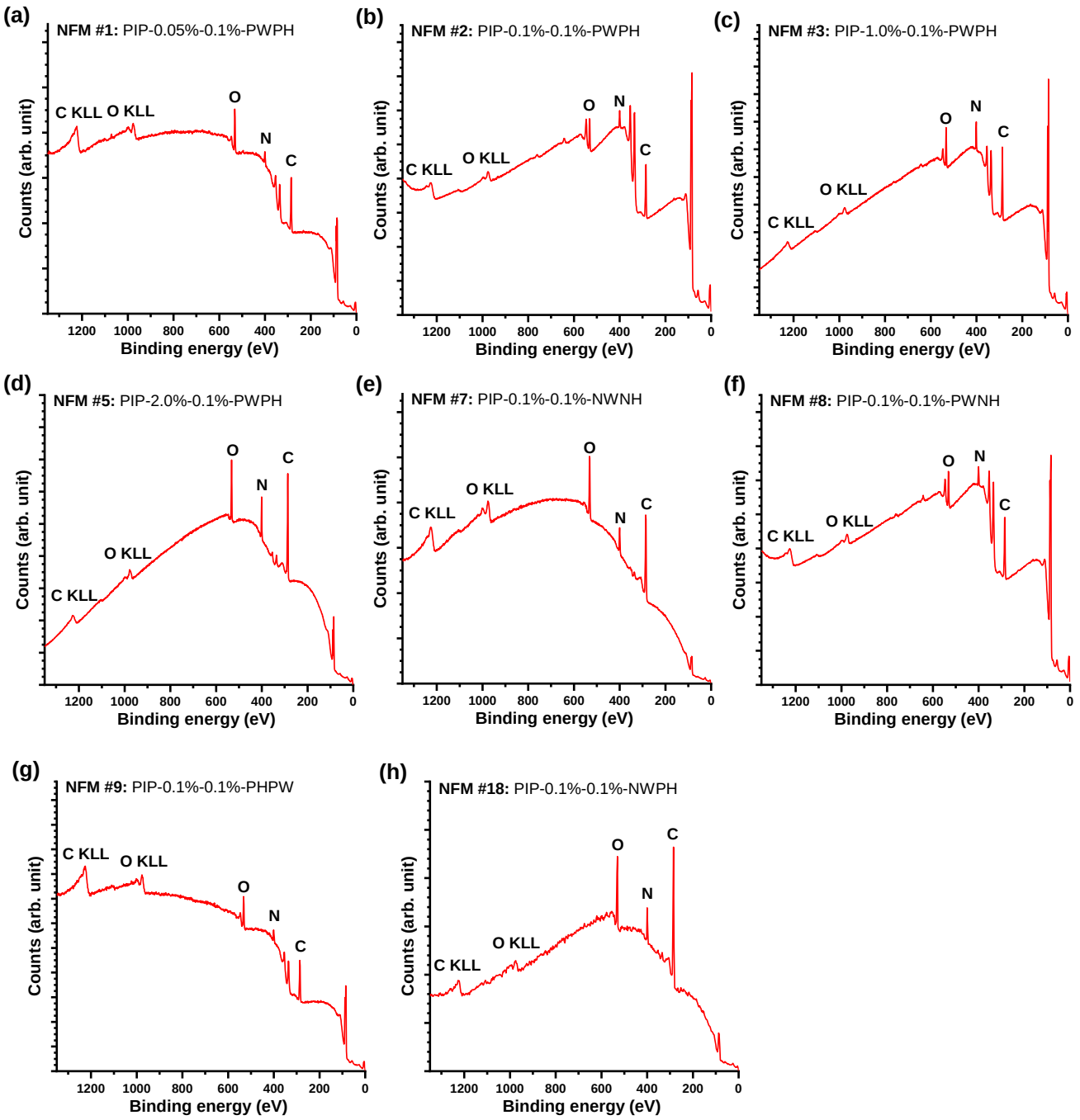

Figure S16: XPS survey spectra of the freestanding polyamide nanofilms transferred onto the gold-coated silicon wafer. (a) For NFM #1 (PIP-0.05%-0.1%-PWPH). (b) For NFM #2 (PIP-0.1%-0.1%-PWPH). (c) For NFM #3 (PIP-1.0%-0.1%-PWPH). (d) For NFM #5 (PIP-2.0%-0.1%-PWPH). (e) For NFM #7 (PIP-0.1%-0.1%-NWNH). (f) For NFM #8 (PIP-0.1%-0.1%-PWNH). (g) For NFM #9 (PIP-0.1%-0.1%-PHPW). (h) For NFM #18 (PIP-0.1%-0.1%-NWPH). PWPH: post-solvent-washing with hexane followed by post-heating at 70 °C for 1 min. NWNH: no solvent-washing and no post-heating. PWNH: post-solvent-washing with hexane and no post-heating. PHPW: post-heating at 70 °C for 1 min followed by post-solvent-washing with hexane. NWPH: no post-solvent-washing and only post-heating at 70 °C for 1 min.

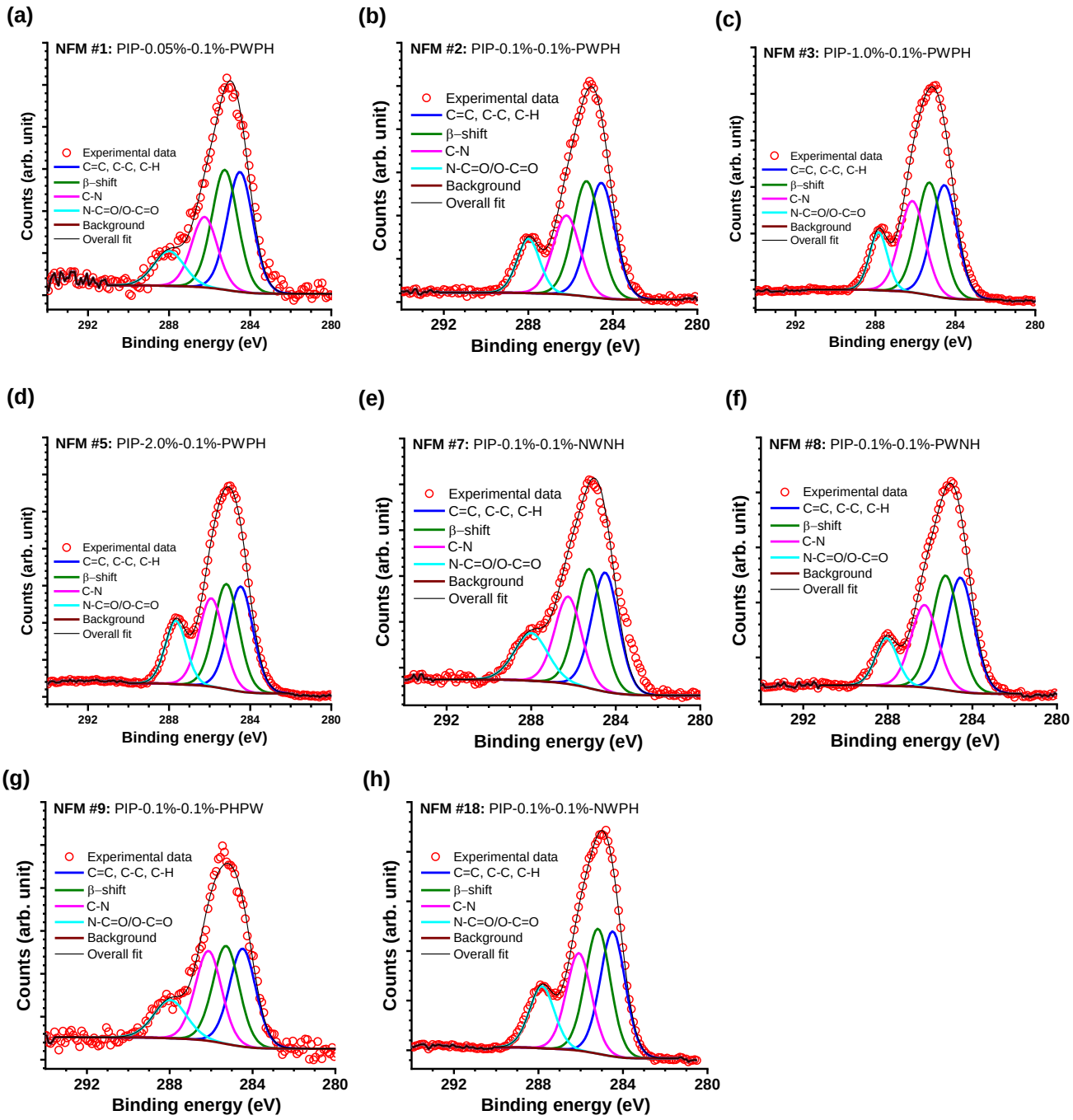

Figure S17: XPS C1s core level spectra of the freestanding polyamide nanofilms transferred onto the gold-coated silicon wafer. (a) For NFM #1 (PIP-0.05%-0.1%-PWPH). (b) For NFM #2 (PIP-0.1%-0.1%-PWPH). (c) For NFM #3 (PIP-1.0%-0.1%-PWPH). (d) For NFM #5 (PIP-2.0%-0.1%-PWPH). (e) For NFM #7 (PIP-0.1%-0.1%-NWNH). (f) For NFM #8 (PIP-0.1%-0.1%-PWNH). (g) For NFM #9 (PIP-0.1%-0.1%-PHPW). (h) For NFM #18 (PIP-0.1%-0.1%-NWPH). PWPH: post-solvent-washing with hexane followed by post-heating at 70 °C for 1 min. NWNH: no solvent-washing and no post-heating. PWNH: post-solvent-washing with hexane and no post-heating. PHPW: post-heating at 70 °C for 1 min followed by post-solvent-washing with hexane. NWPH: no post-solvent-washing and only post-heating at 70 °C for 1 min.

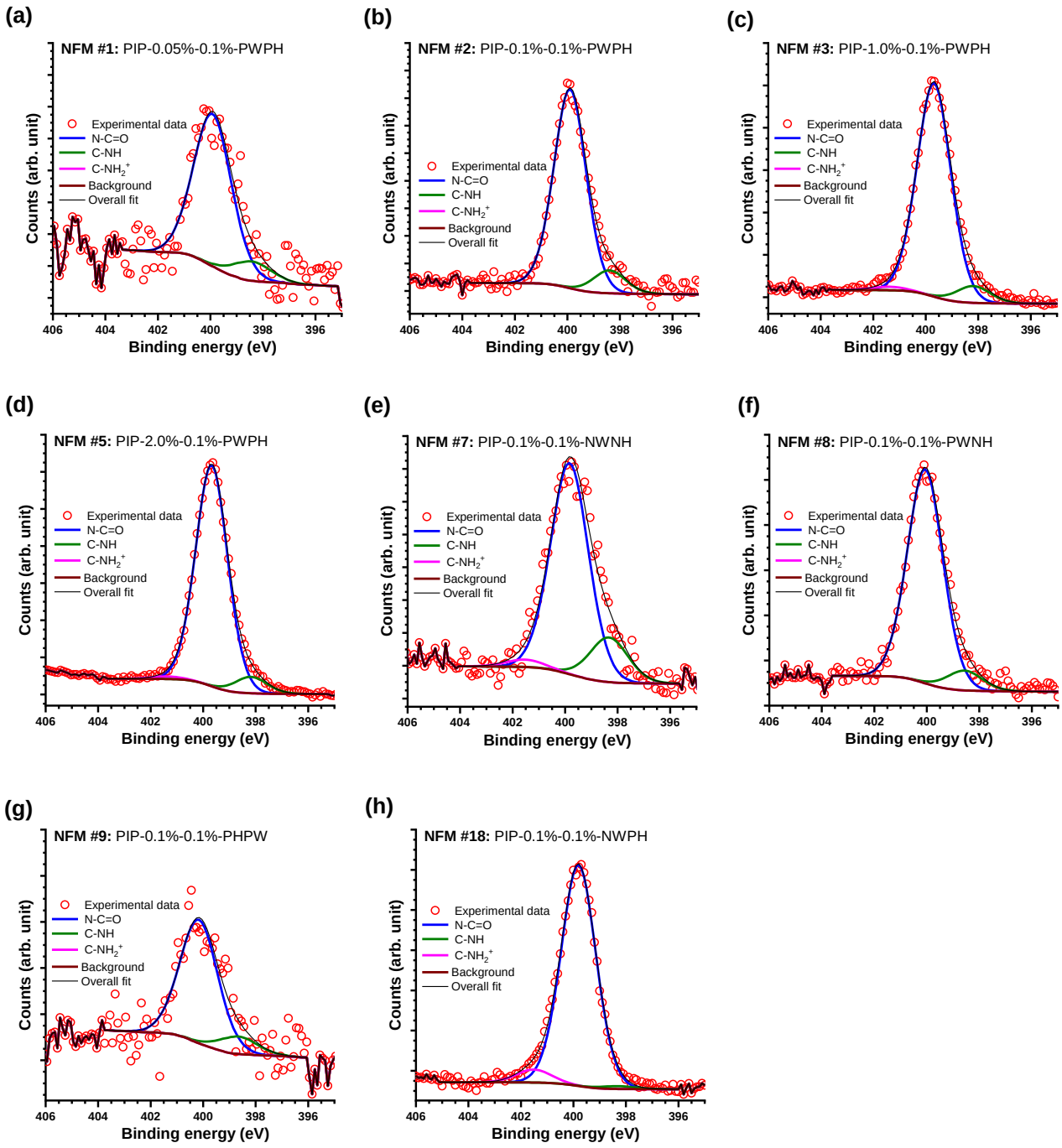

Figure S18: XPS N1s core level spectra of the freestanding polyamide nanofilms transferred onto the gold-coated silicon wafer. (a) For NFM #1 (PIP-0.05%-0.1%-PWPH). (b) For NFM #2 (PIP-0.1%-0.1%-PWPH). (c) For NFM #3 (PIP-1.0%-0.1%-PWPH). (d) For NFM #5 (PIP-2.0%-0.1%-PWPH). (e) For NFM #7 (PIP-0.1%-0.1%-NWNH). (f) For NFM #8 (PIP-0.1%-0.1%-PWNH). (g) For NFM #9 (PIP-0.1%-0.1%-PHPW). (h) For NFM #18 (PIP-0.1%-0.1%-NWPH). PWPH: post-solvent-washing with hexane followed by post-heating at 70 °C for 1 min. NWNH: no solvent-washing and no post-heating. PWNH: post-solvent-washing with hexane and no post-heating. PHPW: post-heating at 70 °C for 1 min followed by post-solvent-washing with hexane. NWPH: no post-solvent-washing and only post-heating at 70 °C for 1 min.

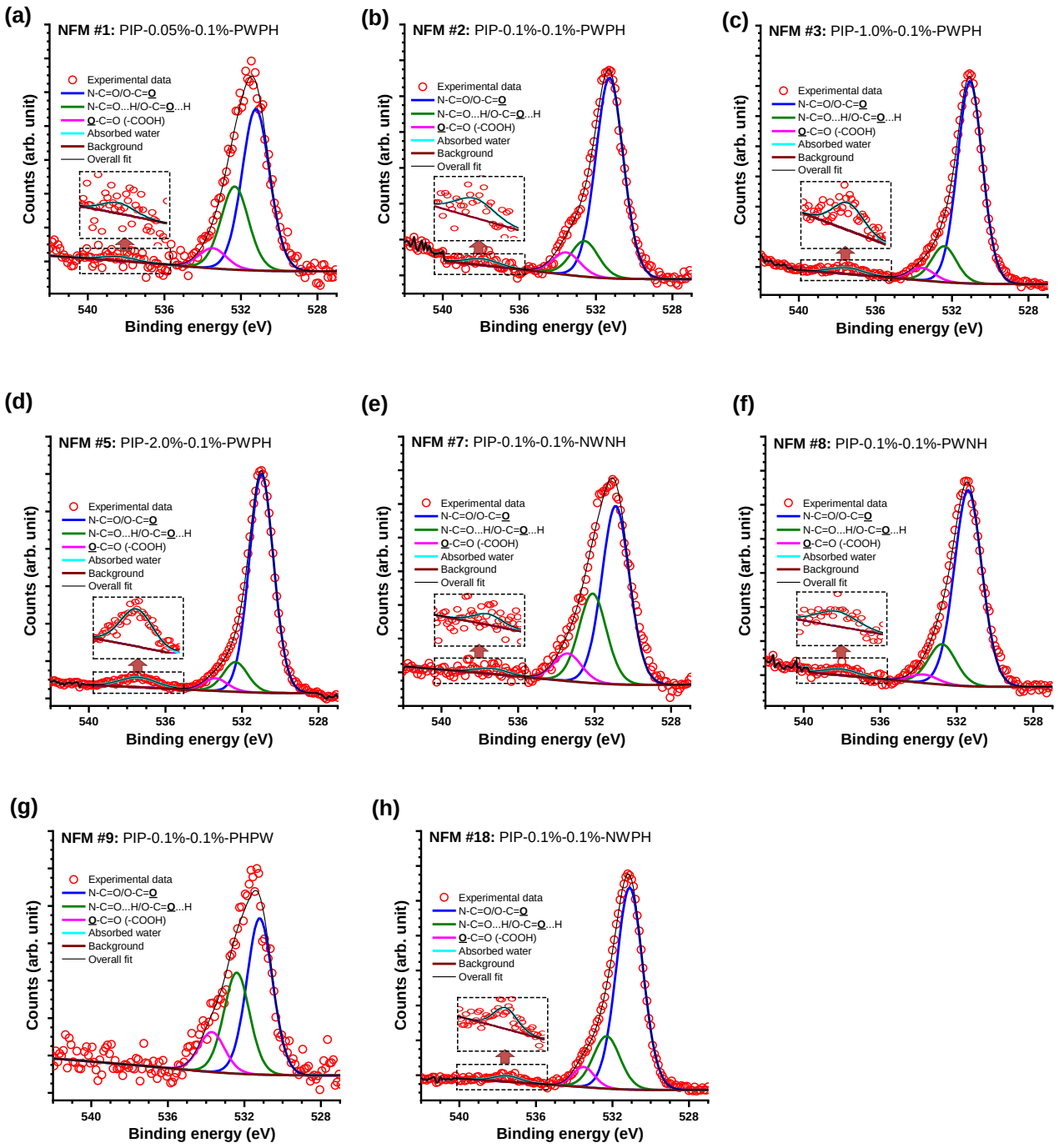

Figure S19: XPS O1s core level spectra of the freestanding polyamide nanofilms transferred onto the gold-coated silicon wafer. (a) For NFM #1 (PIP-0.05%-0.1%-PWPH). (b) For NFM #2 (PIP-0.1%-0.1%-PWPH). (c) For NFM #3 (PIP-1.0%-0.1%-PWPH). (d) For NFM #5 (PIP-2.0%-0.1%-PWPH). (e) For NFM #7 (PIP-0.1%-0.1%-NWNH). (f) For NFM #8 (PIP-0.1%-0.1%-PWNH). (g) For NFM #9 (PIP-0.1%-0.1%-PHPW). (h) For NFM #18 (PIP-0.1%-0.1%-NWPH). PWPH: post-solvent-washing with hexane followed by post-heating at 70 °C for 1 min. NWNH: no solvent-washing and no post-heating. PWNH: post-solvent-washing with hexane and no post-heating. PHPW: post-heating at 70 °C for 1 min followed by post-solvent-washing with hexane. NWPH: no post-solvent-washing and only post-heating at 70 °C for 1 min.

Table S4: Core-level XPS results of the freestanding polyamide nanofilms.

Polyamide nanofilm	C1s			N1s			O1s		
	Energy (eV)	**Species**	**at (%)**	**Energy (eV)**	**Species**	**at (%)**	**Energy (eV)**	**Species**	**at (%)**
NFM #1: PIP-0.05%-0.1%-PWPH	284.5	C=C, C-C, C-H	34.3 ± 1.0	400.0	N-C=O	85.8 ± 2.5	531.2	N-C=O/O-C=**O**	55.0 ± 4.2
	285.2	β – shift	34.3 ± 1.0	398.4	C-NH	14.2 ± 2.5	532.3	N-C=O…H/O-C=**O**…H	35.1 ± 3.7
	286.2	C-N*	20.0 ± 0.8	401.7	$C\text{-}NH_{2+}$	0.0 ± 0.0	533.5	**O**-C=O	8.3 ± 1.1
	288.0	N-C=O/O-C=O	11.4 ± 1.2				538.0	Absorbed water	1.6 ± 0.3
NFM #2: PIP-0.1%-0.1%-PWPH	284.5	C=C, C-C, C-H	32.5 ± 0.3	399.9	N-C=O	88.9 ± 1.0	531.3	N-C=O/O-C=**O**	73.1 ± 2.0
	285.2	β – shift	32.5 ± 0.3	398.4	C-NH	10.8 ± 0.7	532.6	N-C=O…H/O-C=**O**…H	16.8 ± 2.5
	286.2	C-N*	22.4 ± 0.5	401.6	$C\text{-}NH_{2+}$	0.3 ± 0.5	533.5	**O**-C=O	8.4 ± 0.6
	288.0	N-C=O/O-C=O	12.7 ± 0.2				537.9	Absorbed water	1.7 ± 0.8
NFM #3: PIP-1.0%-0.1%-PWPH	284.5	C=C, C-C, C-H	31.4 ± 0.2	399.7	N-C=O	91.5 ± 0.2	531.1	N-C=O/O-C=**O**	77.3 ± 0.7
	285.3	β – shift	31.4 ± 0.2	398.2	C-NH	7.0 ± 0.4	532.4	N-C=O…H/O-C=**O**…H	15.2 ± 1.3
	286.1	C-N*	25.6 ± 1.0	401.4	$C\text{-}NH_{2+}$	1.5 ± 0.3	533.6	**O**-C=O	4.8 ± 0.1
	287.9	N-C=O/O-C=O	11.7 ± 0.6				537.5	Absorbed water	2.7 ± 0.6
NFM #5: PIP-2.0%-0.1%-PWPH	284.5	C=C, C-C, C-H	29.7 ± 0.3	399.6	N-C=O	92.3 ± 0.1	530.9	N-C=O/O-C=**O**	79.4 ± 0.5
	285.2	β – shift	29.7 ± 0.3	398.1	C-NH	6.6 ± 0.4	532.3	N-C=O…H/O-C=**O**…H	11.3 ± 0.8
	285.9	C-N*	25.2 ± 0.3	401.3	$C\text{-}NH_{2+}$	1.2 ± 0.3	533.3	**O**-C=O	4.5 ± 0.4
	287.7	N-C=O/O-C=O	15.5 ± 0.2				537.4	Absorbed water	4.8 ± 0.8
NFM #7: PIP-0.1%-0.1%-NWNH	284.5	C=C, C-C, C-H	29.7 ± 0.9	399.9	N-C=O	79.0 ± 1.7	530.9	N-C=O/O-C=**O**	60.0 ± 0.9
	285.3	β – shift	29.7 ± 0.9	398.4	C-NH	18.7 ± 2.1	532.1	N-C=O…H/O-C=**O**…H	28.7 ± 0.9
	286.3	C-N*	24.1 ± 1.4	401.6	$C\text{-}NH_{2+}$	2.3 ± 0.6	533.4	**O**-C=O	9.2 ± 0.3
	288.0	N-C=O/O-C=O	16.5 ± 1.3				537.8	Absorbed water	2.2 ± 0.2
NFM #8: PIP-0.1%-0.1%-PWNH	284.5	C=C, C-C, C-H	32.4 ± 0.4	400.1	N-C=O	91.8 ± 0.3	531.4	N-C=O/O-C=**O**	78.0 ± 0.4
	285.2	β – shift	32.4 ± 0.4	398.6	C-NH	8.1 ± 0.4	532.7	N-C=O…H/O-C=**O**…H	16.2 ± 0.3
	286.2	C-N*	24.0 ± 0.7	401.8	$C\text{-}NH_{2+}$	0.1 ± 0.1	533.8	**O**-C=O	3.4 ± 0.1
	288.1	N-C=O/O-C=O	11.1 ± 0.1				538.0	Absorbed water	2.4 ± 0.7

NFM #9: PIP-0.1%-0.1%-PHPW	284.5	C=C, C-C, C-H	30.4 ± 1.3	400.1	N-C=O	87.9 ± 2.9	531.2	N-C=O/O-C=**O**	54.3 ± 2.8
	285.3	β – shift	30.4 ± 1.3	398.6	C-NH	11.7 ± 2.8	532.4	N-C=O…H/O-C=**O**…H	33.9 ± 2.4
	286.2	C-N*	25.2 ± 1.9	401.8	$C\text{-}NH_{2+}$	0.4 ± 0.5	533.7	**O**-C=O	11.2 ± 1.8
	288.0	N-C=O/O-C=O	13.9 ± 1.0				538.1	Absorbed water	0.5 ± 0.4
NFM #18: PIP-0.1%-0.1%-NWPH	284.5	C=C, C-C, C-H	30.8 ± 0.9	399.8	N-C=O	93.3 ± 1.0	531.2	N-C=O/O-C=**O**	71.9 ± 3.0
	285.2	β – shift	30.8 ± 0.9	398.3	C-NH	1.4 ± 0.3	532.4	N-C=O…H/O-C=**O**…H	18.8 ± 1.2
	286.1	C-N*	23.2 ± 1.4	401.5	$C\text{-}NH_{2+}$	5.4 ± 0.8	533.6	**O**-C=O	6.9 ± 1.7
	287.9	N-C=O/O-C=O	15.2 ± 0.6				537.6	Absorbed water	2.5 ± 0.4

PWPH: post-solvent-washing with hexane and post-heating at 70 °C for 1 min. NWNH: no post-solvent-washing and no post-heating. PWNH: post-solvent-washing with hexane and no post-heating. PHPW: post-heating at 70 °C for 1 min and post-solvent-washing with hexane. NWPH: no post-solvent-washing and only post-heating at 70 °C for 1 min. *C-N: C-N-C=O, C-NH, $C\text{-}NH_2^+$

Zeta potential measurement of the nanofilm composite membranes

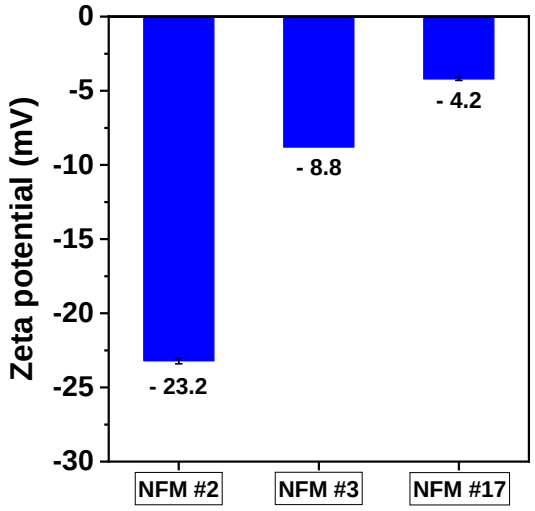

Figure S20: Surface zeta potential of the nanofilm composite membranes prepared on HPAN support. NFM #2: PIP-0.1%-0.1%-PWPH, NFM #3: PIP-1.0%-0.1%-PWPH and NFM #17: PIP-3.0%-0.1%-PWPH. PWPH: post-solvent-washing with hexane and post-heating at 70 °C for 1 min.

Nanofiltration performance

Nanofiltration performance of the nanofilm composite membranes fabricated on HPAN support

The desalination performance of the nanofilm composite membrane was tested in a cross-flow filtration system. Circular membrane samples were used in each testing cell with an effective surface area of 14.5 cm^2. Unless stated otherwise, all experiments were performed under 5 bar applied pressure with 2 g L^{-1} salt concentration as feed solution and maintaining the feed temperature at 25 (±1) °C. All results were collected after allowing the membrane to reach a steady state, which was achieved by waiting for ~7 hours under cross-flow at 5 bar pressure. A minimum of four membrane coupons from each membrane sheet was tested to calculate the standard deviation in permeance and salt rejection values. The permeance of the membrane was calculated from the following equation (S4):

$$\mathrm{P}\ (\mathrm{L}\, m^{-2} h^{-1} bar^{-1}) = \frac{\mathrm{V}}{\mathrm{A}.t.\Delta p} \quad \ldots\ldots\ldots\ldots\ldots \text{(S4)}$$

where V is the volume of the permeate (liter), A is the membrane surface area (m^2), and t is the time (hour) required to collect the volume V under a trans-membrane pressure of Δp.

The rejection of salts, dyes, and neutral solutes was calculated from the following equation (S5):

$$Rejection\ (\%) = \frac{C_f(feed) - C_p(permeate)}{C_f(feed)} \times 100\ \% \quad \text{.....(S5)}$$

where *Cp* is the concentration of dissolved salt/solute in the permeate and C_f is the concentration of dissolved salt/solute in the feed.

The ion (or solute) selectivity was calculated from the following equation (S6):

$$Selectivity = \frac{100 - rejection\ of\ 1^{st}\ ion\ (or\ solute)}{100 - rejection\ of\ 2^{st}\ ion\ (or\ solute)} \text{ ..... (S6)}$$

Table S5: Desalination performance of the nanofilm composite membrane (NFM #1: PIP-0.05%-0.1%-PWPH). Batch 1, Batch 2, Batch 3, and Batch 4 were fabricated on HPAN support under identical monomer concentrations, post-solvent-washing, and heat-treatment methods.

NFM #1: PIP-0.05%-0.1%-PWPH					
Membrane	**Pure water permeance (L m^{-2} h^{-1} bar^{-1})**	**Na_2SO_4**		**NaCl**	
		Water permeance (L m^{-2} h^{-1} bar^{-1})	**Rejection (%)**	**Water permeance (L m^{-2} h^{-1} bar^{-1})**	**Rejection (%)**
		Batch 1			
Coupon 1	71.3	34.6	96.5	56.5	9.1
Coupon 2	77.3	36.4	92.9	60.3	8.3
Coupon 3	67.5	32.2	98.8	54.8	11.2
Coupon 4	73.8	33.4	94.3	56.5	6.7
		Batch 2			
Coupon 1	66.7	27.6	95.2	56.5	9.8
Coupon 2	62.7	27.7	96.3	54.9	10.7
Coupon 3	66.1	26.1	94.1	57.1	8.1
		Batch 3			
Coupon 1	73.6	30.6	97.4	ND	ND
		Batch 4			
Coupon 1	63.7	29.2	96.6	57.4	11.6
Coupon 2	62.8	28.0	96.9	55.8	10.9
Coupon 3	62.6	28.0	97.2	53.8	12.1
Average	**68.0 ± 5.2**	**30.3 ± 3.3**	**96.0 ± 1.7**	**56.4 ± 1.8**	**9.8 ± 1.8**

* ND: Not determined

Table S6: Nanofiltration performance of the nanofilm composite membranes fabricated on HPAN support.

Nanofilm composite Membranes	Nanofiltration performance of the membrane					
	Feed →	**Pure water**	**Na_2SO_4**	**$MgSO_4$**	**$MgCl_2$**	**NaCl**
NFM #1: PIP-0.05%-0.1%-PWPH	Water permeance (L m^{-2} h^{-1} bar^{-1})	68.0 ± 5.2	30.3 ± 3.3	37.0 ± 2.6	53.4 ± 2.1	56.4 ± 1.8
	Salt rejection (%)	---	96.0 ± 1.7	84.8 ± 6.5	16.4 ± 2.5	9.8 ± 1.8
NFM #20: PIP-0.05%-0.1%-PWPH[a]	Water permeance (L m^{-2} h^{-1} bar^{-1})	63.7 ± 4.0	30.3 ± 1.1	56.9 ± 1.3	56.7 ± 4.0	55.9 ± 3.1
	Salt rejection (%)	---	98.8 ± 0.3	85.5 ± 1.3	11.0 ± 2.7	10.3 ± 1.2
NFM #21: PIP-0.05%-0.15%-PWPH	Water permeance (L m^{-2} h^{-1} bar^{-1})	79.5 ± 6.3	33.6 ± 2.6	53.0 ± 6.0	71.6 ± 6.8	62.2 ± 4.7
	Salt rejection (%)	---	81.0 ± 6.5	39.9 ± 11.4	4.0 ± 1.8	3.2 ± 0.9
NFM #2: PIP-0.1%-0.1%-PWPH	Water permeance (L m^{-2} h^{-1} bar^{-1})	61.3 ± 2.6	32.9 ± 1.8	36.3 ± 2.1	44.8 ± 2.1	50.6 ± 1.6
	Salt rejection (%)	---	99.46 ± 0.10	94.8 ± 0.7	27.7 ± 0.5	11.9 ± 0.8
NFM #22: PIP-0.1%-0.15%-PWPH	Water permeance (L m^{-2} h^{-1} bar^{-1})	60.2 ± 2.2	29.0 ± 1.4	40.5 ± 0.9	49.3 ± 0.6	47.5 ± 0.7
	Salt rejection (%)	---	98.5 ± 0.5	89.8 ± 3.1	26.8 ± 1.8	10.3 ± 3.4
NFM #3: PIP-1.0%-0.1%-PWPH	Water permeance (L m^{-2} h^{-1} bar^{-1})	37.1 ± 2.0	24.6 ± 1.4	27.2 ± 1.3	23.3 ± 1.4	32.5 ± 1.5
	Salt rejection (%)	---	99.76 ± 0.13	99.1 ± 0.4	93.5 ± 0.94	25.1 ± 3.8
NFM #23: PIP-1.0%-0.15%-PWPH	Water permeance (L m^{-2} h^{-1} bar^{-1})	49.6 ± 0.8	26.4 ± 0.6	33.0 ± 0.7	28.4 ± 0.8	39.8 ± 0.9
	Salt rejection (%)	---	99.37 ± 0.20	98.3 ± 0.2	83.2 ± 1.1	12.3 ± 2.0
NFM #24: PIP-1.0%-0.15%-PWPH[b]	Water permeance (L m^{-2} h^{-1} bar^{-1})	54.1 ± 1.3	26.7 ± 0.1	51.0 ± 1.9	46.5 ± 3.0	47.9 ± 0.5
	Salt rejection (%)	---	98.7 ± 0.3	90.2 ± 1.3	19.4 ± 3.8	11.1 ± 0.7
NFM #4: PIP-2.0%-0.05%-PWPH	Water permeance (L m^{-2} h^{-1} bar^{-1})	23.2 ± 1.7	16.7 ± 1.0	18.3 ± 1.2	15.2 ± 1.0	19.7 ± 1.5
	Salt rejection (%)	---	99.69 ± 0.01	99.7 ± 0.1	98.5 ± 0.1	36.6 ± 1.8
NFM #5: PIP-2.0%-0.1%-PWPH	Water permeance (L m^{-2} h^{-1} bar^{-1})	30.1 ± 2.6	20.1 ± 1.1	21.1 ± 1.1	17.7 ± 0.8	24.8 ± 1.5
	Salt rejection (%)	---	99.82 ± 0.04	99.7 ± 0.1	98.0 ± 0.2	28.3 ± 2.0
NFM #6: PIP-2.0%-0.15%-PWPH	Water permeance (L m^{-2} h^{-1} bar^{-1})	38.4 ± 1.3	22.1 ± 0.3	24.9 ± 0.4	20.8 ± 0.4	31.5 ± 1.3
	Salt rejection (%)	---	99.70 ± 0.10	99.2 ± 0.4	93.2 ± 1.0	19.1 ± 2.0
Dow FILMTEC™ NF270 (tested in our laboratory)[b]	Water permeance (L m^{-2} h^{-1} bar^{-1})	22.2 ± 1.5	19.0 ± 1.7	15.2 ± 0.2	14.0 ± 0.1	17.8 ± 1.4
	Salt rejection (%)	---	99.56 ± 0.10	99.1 ± 0.3	59.7 ± 1.8	51.5 ± 2.2

PWPH: post-solvent-washing with hexane and post-heating at 70 °C for 1 min. [a]Interfacial polymerization time was 60 s. [b]data taken from ref. 1.

Table S7: Nanofiltration performance of the nanofilm composite membranes fabricated on HPAN support. 1 mM sodium lauryl sulfate (SLS) was added in the aqueous phase during interfacial polymerization.

Nanofilm composite Membranes	Nanofiltration performance of the membrane					
	Feed →	**Pure water**	**Na_2SO_4**	**$MgSO_4$**	**$MgCl_2$**	**NaCl**
PIP-0.05%+1 mM SLS-0.1%-NWPH* (Thickness: 12.1 nm)	Water permeance (L m^{-2} h^{-1} bar^{-1})	23.1 ± 1.7	17.4 ± 1.1	18.0 ± 1.0	15.6 ± 1.0	20.5 ± 1.7
	Salt rejection (%)	---	99.95 ± 0.03	99.6 ± 0.1	93.9 ± 2.7	45.0 ± 0.3
PIP-0.05%+1 mM SLS-0.1%-PWPH	Water permeance (L m^{-2} h^{-1} bar^{-1})	29.8 ± 2.4	17.4 ± 0.8	---	18.4 ± 0.8	---
	Salt rejection (%)	---	99.54 ± 0.25	---	96.7 ± 0.3	---
PIP-0.1%+1 mM SLS-0.1%-NWPH* (Thickness: 20.6 nm)	Water permeance (L m^{-2} h^{-1} bar^{-1})	16.4 ± 1.1	12.4 ± 0.8	12.4 ± 1.3	12.6 ± 0.7	13.7 ± 1.0
	Salt rejection (%)	---	99.96 ± 0.03	99.8 ± 0.1	98.1 ± 0.1	42.1 ± 1.8
PIP-0.1%+1 mM SLS-0.1%-PWPH	Water permeance (L m^{-2} h^{-1} bar^{-1})	21.1 ± 0.4	15.1 ± 0.2	16.6 ± 0.2	14.3 ± 0.2	17.6 ± 0.3
	Salt rejection (%)	---	99.68 ± 0.07	99.7 ± 0.1	98.1 ± 0.3	33.3 ± 1.9

*data are taken from ref.1. NWPH: no post-solvent-washing with hexane and only post-heating at 70 °C for 1 min. PWPH: post-solvent-washing with hexane and post-heating at 70 °C for 1 min.

Table S8: Nanofiltration performance of the nanofilm composite membrane (NFM #2: PIP-0.1%-0.1%-PWPH) fabricated on HPAN support. Repeated post-solvent-washing was done followed by post-heating at 70 °C for 1 min.

Post-solvent-washing	Nanofiltration performance of the membrane					
	Feed →	**Pure water**	**Na_2SO_4**	**$MgSO_4$**	**$MgCl_2$**	**NaCl**
Hexane followed by water	Water permeance (L m^{-2} h^{-1} bar^{-1})	59.4 ± 2.8	35.2 ± 3.4	39.2 ± 3.2	48.0 ± 3.5	52.1 ± 3.6
	Salt rejection (%)	---	99.43 ± 0.35	95.7 ± 1.4	27.2 ± 2.3	17.5 ± 2.5
Hexane followed by methanol and then water	Water permeance (L m^{-2} h^{-1} bar^{-1})	61.1 ± 0.5	35.3 ± 1.8	40.9 ± 1.7	47.1 ± 5.7	54.9 ± 0.6
	Salt rejection (%)	---	99.36 ± 0.23	96.5 ± 0.2	33.0 ± 3.6	17.9 ± 1.6
Hexane followed by acetonitrile and then water	Water permeance (L m^{-2} h^{-1} bar^{-1})	54.9 ± 3.8	33.6 ± 3.6	44.7 ± 13.1	44.2 ± 4.6	48.8 ± 5.1
	Salt rejection (%)	---	99.34 ± 0.23	95.9 ± 0.8	37.8 ± 4.6	16.2 ± 0.7
Hexane followed by heptane and then water	Water permeance (L m^{-2} h^{-1} bar^{-1})	56.3 ± 1.5	33.5 ± 1.5	43.2 ± 11.8	46.1 ± 2.0	51.6 ± 1.9
	Salt rejection (%)	---	99.40 ± 0.19	95.6 ± 1.1	29.7 ± 2.9	16.9 ± 0.9

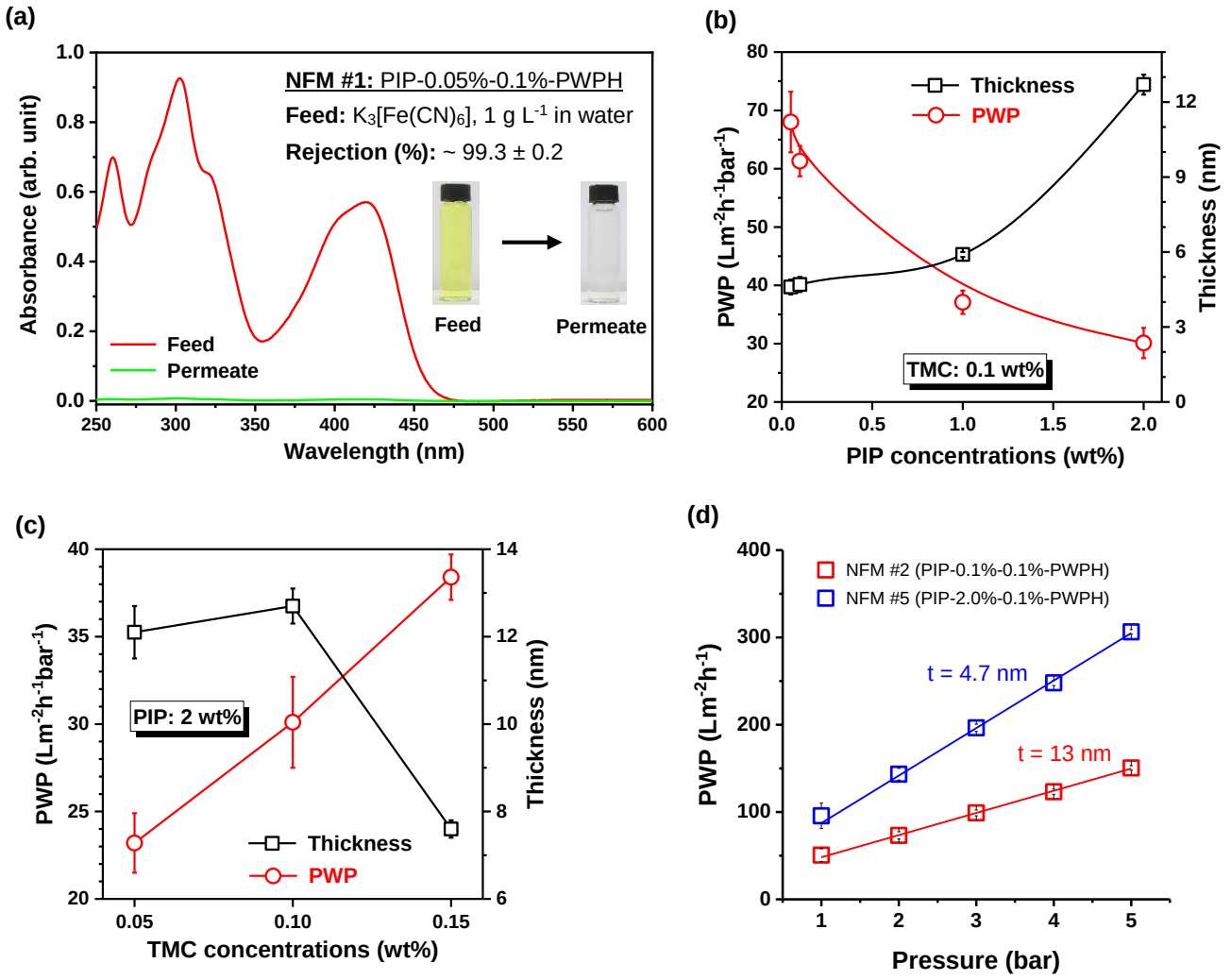

Figure S21: (a) UV-absorbance spectra of potassium ferricyanide ($K_3[Fe(CN)_6]$) measured from the aqueous feed and permeate of the nanofilm composite membrane (NFM #1: PIP-0.05%-0.1%-PWPH). Inset images show the photograph of the aqueous feed and permeate. (b) Variation of the thickness of the nanofilm and the pure water permeance of the membrane with varying concentrations of PIP (TMC: 0.1 wt%). (c) Variation of the thickness of the nanofilm and the pure water permeance of the membrane with varying concentrations of TMC (PIP: 2.0 wt%). (d) The plot of pure water permeance with increasing applied pressure across the membranes. Steady-state water permeance was measured at 5 bar and the subsequent permeances were measured by reducing the pressure from 5 to 1 bar.

Formation of polyamide nanofilm at the interface and our hypothesis on the post-treatment of the nascent nanofilm

Our hypothesis on the formation of polyamide nanofilm via interfacial polymerization is summarized below. We have considered mainly two situations for the growth of the nanofilm. (A) non-stoichiometric equilibrium at the interface and (B) stoichiometric equilibrium at the interface.

(A) Nanofilm formed under non-stoichiometric equilibrium at the interface

The non-stoichiometric equilibrium at the interface arises at a low concentration of PIP and a high concentration of TMC. Loosely crosslinked nascent nanofilm consists of small polyamide clusters is formed in the hexane phase during the interfacial polymerization. This remains as a thermodynamically unstable structure with highly swelled in hexane. The nanofilm gets densified and grows very slowly by additional polymerization with the remaining PIP and TMC trapped inside the nascent nanofilm during drying and post-heating treatment. The growth process stops after the complete evaporation of hexane and hydrolysis of TMC. After complete evaporation of hexane, the nanofilm is further densified through strong intermolecular and intramolecular hydrogen bonding between the amide and carboxylic acid (generated from the hydrolysis of unreacted TMC) groups, respectively. As a result, the thickness of the nanofilm and hence the pore size is reduced. The structure of the final nanofilm is thermodynamically stable. A schematic presentation of the growth mechanism is provided in Figure S22.

(B) Nanofilm formed under stoichiometric equilibrium at the interface

The stoichiometric equilibrium at the interface arises at a high concentration of PIP and a high concentration of TMC. Relatively densely packed and highly crosslinked nascent nanofilm consists of polyamide clusters formed in the hexane phase during the polymerization. The nanofilm does not grow much during the drying and post-heating treatment as compared to the nanofilm formed under non-stoichiometric equilibrium. After complete evaporation of hexane, a thermodynamically stable nanofilm is produced through strong intermolecular and intramolecular hydrogen bonding between

the amide and carboxylic acid (generated from the hydrolysis of unreacted TMC) groups, respectively. The thickness and the pore size of the nanofilm do not reduce significantly in the final structure after post-heating treatment. A schematic presentation of the growth mechanism is provided in Figure S22.

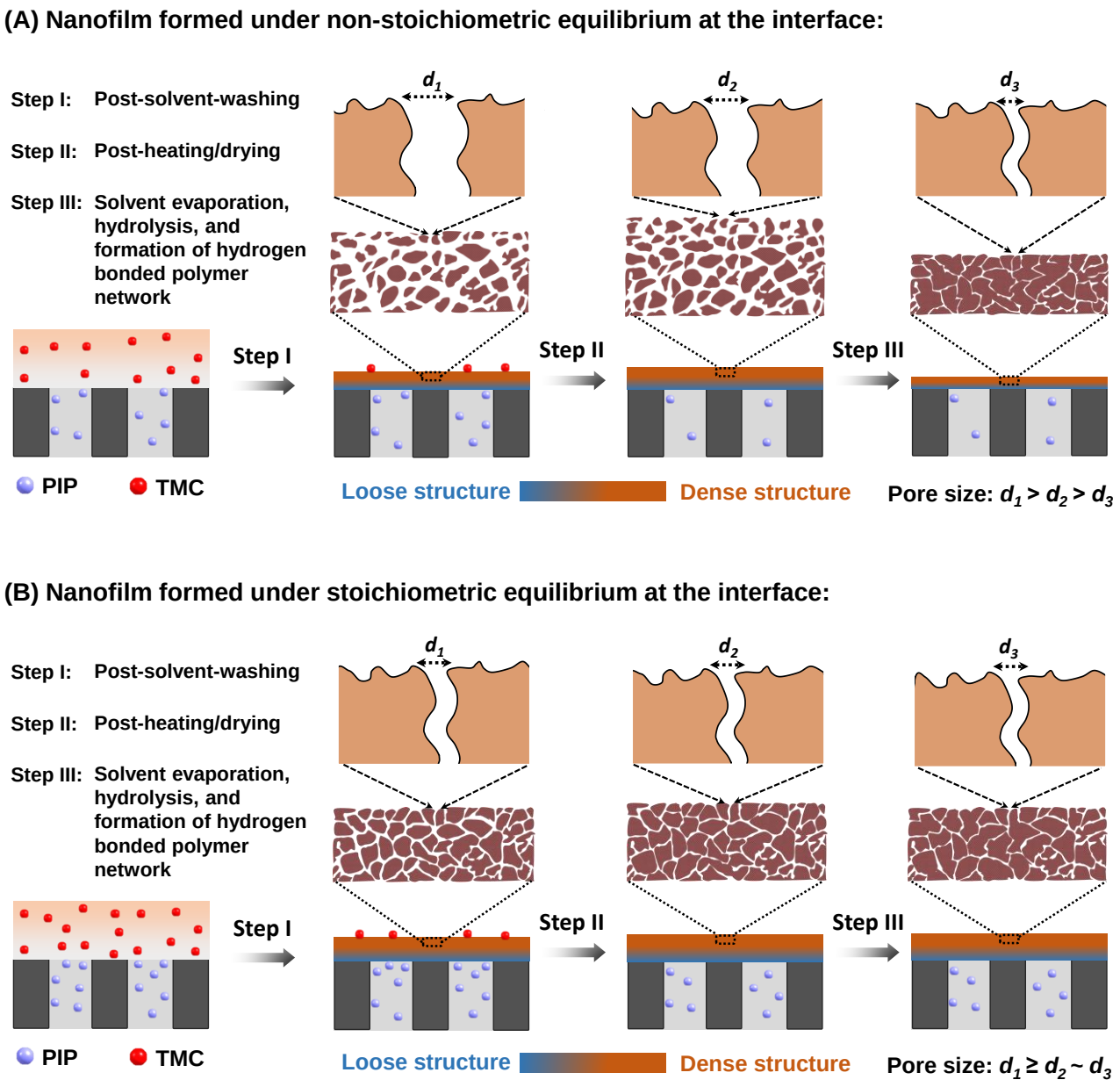

Figure S22: Schematic presentation of the formation of polyamide nanofilm via interfacial polymerization. (A) Nanofilm formed under non-stoichiometric equilibrium at the interface. (B) Nanofilm formed under stoichiometric equilibrium at the interface.

Dependence of the permeance with liquid viscosity

Table S9: Permeance of polyamide nanofilms composite membranes fabricated on HPAN support, measured for different viscosity of the feed solution.

Feed solution	Viscosity (cP)	Nanofilm composite membranes	
		NFM #2 PIP-0.1%-0.1%-PWPH	NFM #5 PIP-2.0%-0.1%-PWPH
		Permeance ($Lm^{-2}h^{-1}bar^{-1}$)	Permeance ($Lm^{-2}h^{-1}bar^{-1}$)
Pure water @ 25 °C	0.89	61.27 ± 2.5	30.05 ± 2.6
Pure water @ 20 °C	1.00	52.69 ± 1.5	26.77 ± 2.3
Pure water @ 15 °C	1.14	45.27 ± 1.3	22.67 ± 1.8
MeOH : Water (1:9 by v/v %) @ 25 °C	1.21	44.05 ± 0.8	23.08 ± 1.7
MeOH : Water (1:9 by v/v %) @ 20 °C	1.32	36.28 ± 0.6	18.58 ± 1.2
MeOH : Water (1:4 by v/v %) @ 25 °C	1.43	36.06 ± 0.8	18.60 ± 1.4
MeOH : Water (1:4 by v/v %) @ 20 °C	1.60	32.19 ± 0.9	15.15 ± 1.5
MeOH : Water (1:4 by v/v %) @ 15 °C	1.82	26.86 ± 0.8	12.05 ± 0.9

PWPH: Post-solvent-washing with hexane and post-heating at 70 °C for 1 min. Feed with varying viscosity was adjusted by varying water-methanol composition at different temperatures.

Table S10. Measurement of ion selectivity (Cl^- to SO_4^{2-} and Na^+ to Mg^{2+}) from mixed salt.

Polyamide nanofilms (amine wt%-TMC wt%-post-treatment)	Selectivity (Cl^- to SO_4^{2-}) in a single salt	Feed I			Feed II			Mixed ion selectivity (Cl^- to SO_4^{2-})	Mixed ion selectivity (Na^+ to Mg^{2+})
		WP (LMH bar)	Rejection of SO_4^{2-} (%)	Rejection of Cl^- (%)	WP (LMH bar)	Rejection of Mg^{2+} (%)	Rejection of Na^+ (%)		
NFM #3: PIP-1.0%-0.1%-PWPH	312.0	29.2 ± 1.3	99.82 ± 0.12	13.9 ± 7.5	28.6 ± 1.4	94.23 ± 1.2	-36.1 ± 5.8	478.3	23.6
NFM #4: PIP-2.0%-0.05%-PWPH	204.5	18.7 ± 1.4	99.94 ± 0.01	24.6 ± 3.1	17.3 ± 1.1	99.57 ± 0.16	-6.2 ± 5.8	1256.6	246.9
NFM #5: PIP-2.0%-0.1%-PWPH	398.0	23.0 ± 1.3	99.93 ± 0.01	12.5 ± 2.9	20.8 ± 1.1	99.19 ± 0.13	-22.0 ± 5.9	1250.0	150.6
NFM #6: PIP-2.0%-0.15%-PWPH	269.7	28.7 ± 0.7	99.53 ± 0.44	-7.1 ± 4.9	25.4 ± 0.6	95.0 ± 0.9	1.2 ± 3.4	228.0	19.8

PWPH: post-solvent-washing with hexane and post-heating at 70 °C for 1 min.

Table S11. Measurement of ion rejection and selectivity from synthetic seawater.

Polyamide nanofilms (amine wt%-TMC wt%-post-treatment)	Membrane performance in seawater						Ion selectivity (Cl^- to SO_4^{2-})	Ion selectivity (Na^+ to Mg^{2+})
	PWP (LMH bar) at 10 bar	WP (LMH bar)	Rejection of SO_4^{2-} (%)	Rejection of Cl^- (%)	Rejection of Mg^{2+} (%)	Rejection of Na^+ (%)		
NFM #3: PIP-1.0%-0.1%-PWPH	33.0 ± 1.1	9.5 ± 0.4	98.79 ± 0.53	18.6 ± 1.6	94.3 ± 0.9	7.2 ± 2.1	67.3	16.3
NFM #4: PIP-2.0%-0.05%-PWPH	22.0 ± 1.5	5.6 ± 0.3	99.84 ± 0.06	23.2 ± 2.3	98.86 ± 0.02	9.4 ± 0.8	480	79.5
NFM #5: PIP-2.0%-0.1%-PWPH	25.7 ± 1.6	6.2 ± 0.3	99.35 ± 0.49	21.7 ± 1.5	97.9 ± 0.6	10.4 ± 1.4	120.5	42.7

PWPH: post-solvent-washing with hexane and post-heating at 70 °C for 1 min. Nanofiltration performance in synthetic seawater condition (used salts concentration are NaCl: 24.5 g L^{-1}, $MgCl_2$: 5.2 g L^{-1}, Na_2SO_4: 4.09 g L^{-1}, $CaCl_2$: 1.16 g L^{-1} and KCl: 0.695 g L^{-1}). Membranes were tested at 25 (±1) °C under 10 bar applied pressure and 50 L h^{-1} cross-flow.

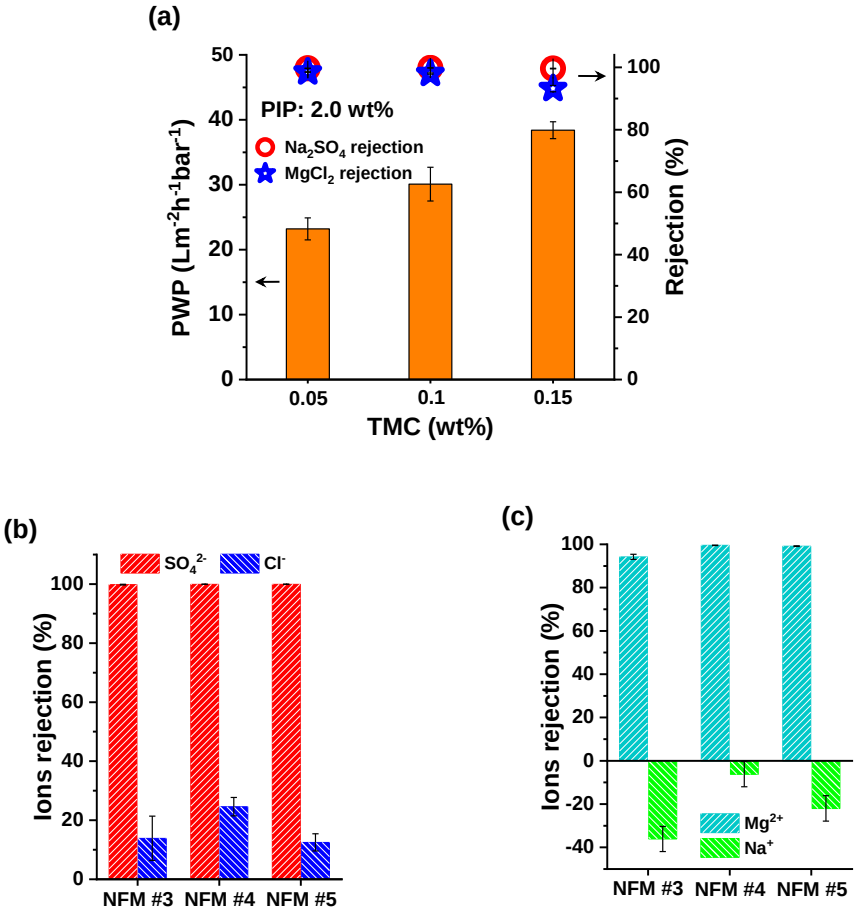

Figure S23: Nanofiltration performance of the polyamide nanofilms composite membranes fabricated on HPAN support. (a) The plot of pure water permeance, Na_2SO_4 rejection, and $MgCl_2$ rejection at a constant PIP concentration of 2.0 wt% in the aqueous phase against different TMC (wt%) concentrations in the hexane phase. (b and c) Ions (SO_4^{2-}, Cl^-, Mg^{2+}, and Na^+) rejection from different nanofilm composite membranes. Two salts were mixed with equal concentrations (1 g L^{-1} each) and used as feed. For SO_4^{2-} and Cl^- ions rejection, Na_2SO_4 and NaCl mixed solution was used as feed. For Mg^{2+} and Na^+ ions, $MgCl_2$ and NaCl mixed solution was used as feed. Membranes were tested under 5 bar applied pressure at 25 (±1) °C temperature with 50 L h^{-1} cross-flow velocity.

Table S12. Pure water permeance (PWP), rejection of Na_2SO_4 (2 g L^{-1}) and NaCl (2 g L^{-1}), and the single salt selectivity between NaCl to Na_2SO_4 of the nanofilm composite membranes.

Polyamide nanofilms (amine wt%-TMC wt%-post-treatment)	**PWP (LMH bar) at 5 bar**	**Rejection of Na_2SO_4 (%)**	**Rejection of NaCl (%)**	**Selectivity (NaCl to Na_2SO_4) in a single salt**
NFM #1: PIP-0.05%-0.1%-PWPH	68.0 ± 5.2	96.0 ± 1.7	9.8 ± 1.8	22.6
NFM #2: PIP-0.1%-0.1%-PWPH	61.3 ± 2.6	99.46 ± 0.10	11.9 ± 0.8	163
NFM #3: PIP-1.0%-0.1%-PWPH	37.1 ± 2.0	99.76 ± 0.13	25.1 ± 3.8	312
NFM #4: PIP-2.0%-0.05%-PWPH	23.2 ± 1.7	99.69 ± 0.01	36.6 ± 1.8	204.5
NFM #5: PIP-2.0%-0.1%-PWPH	30.1 ± 2.6	99.82 ± 0.04	28.3 ± 2.0	398.3
NFM #6: PIP-2.0%-0.15%-PWPH	38.4 ± 1.3	99.70 ± 0.10	19.1 ± 2.0	270
NFM #20: PIP-0.05%-0.1%-PWPH[a]	63.7 ± 4.0	98.83 ± 0.3	10.3 ± 1.2	76.7
NFM #21: PIP-0.05%-0.15%-PWPH	79.5 ± 6.3	81.09 ± 6.53	3.2 ± 0.9	5.12
NFM #22: PIP-0.1%-0.15%-PWPH	60.2 ± 2.2	98.55 ± 0.47	10.3 ± 3.4	61.9
NFM #23: PIP-1.0%-0.15%-PWPH	49.6 ± 0.8	99.37 ± 0.2	12.3 ± 2.0	139.2
NFM #24: PIP-1.0%-0.15%-PWPH[a]	54.1 ± 1.3	98.70 ± 0.3	11.1 ± 0.7	68.4

PWPH: post-solvent-washing with hexane and post-heating at 70 °C for 1 min. [a]Interfacial polymerization time was 60 s.

Table S13: List of literature data to calculate ideal salt selectivity [NaCl to Na_2SO_4].

Membranes and their description	Membrane code/ Abbreviation used in the reference	#PWP	Salt rejection (%)		Single salt selectivity [NaCl to Na_2SO_4]	Reference
			Na_2SO_4	NaCl		
Sulfonated polyamide TFC membranes with improved water flux	Piperazine (PIP)	12.9	95.8	38.8	14.6	1. *Desalination* **377,** 11–22 (2016).
	2,5-DABSA + PIP	20.4	97.2	37.6	22.3	
Chlorine-tolerant NF membranes from piperazine and BHTTM	before oxidation	8.7	99.5	NA	NA	2. *J. Membr. Sci.* **498,** 374–384 (2016).
	after oxidation	13.2	99.5	30.0	140	
Commercial membranes	DOW FILMTEC™ NF70	7.2	[a]97.0	70.0	10.0	2. *J. Membr. Sci.* **498,** 374–384 (2016).
	DOW FILMTEC™ NF90	6.7	[a]98.0	90.0	5.0	
	GE-Osmonics DL	10.0	[a]96.0	40.0	15.0	
	GE-Osmonics HL	6.9	[a]97.0	33.0	23.3	
	Synder NFX	2.4	[a]99.0	40.0	60.0	
	Synder NFW	5.4	[a]97.0	20.0	26.7	
Sericin incorporated poly(piperazineamide) NF membrane for enhanced perm-selectivity and fouling resistance	Sericin 0.0 wt%	12.0	97.2	40.6	21.2	3.. *J. Membr. Sci.* **523,** 282–290 (2017).
	Sericin 0.03 wt%	14.8	97.2	35.3	23.1	
	Sericin 0.06 wt%	16.4	97.3	32.0	25.2	
	Sericin 0.09 wt%	16.7	95.8	26.3	17.5	
Carboxylic monoamines incorporated TFC polyamide membranes	Piperazine (PIP)	5.8	95.3	29.9	14.9	4. *J. Membr. Sci.* **539,** 52–64 (2017).
	PIP + ABA	11.9	93.2	15.6	12.4	
Chlorine-tolerant polypiperazine-amide NF membrane by adding NH_2-PEG-NH_2	Piperazine (PIP)	5.3	98.3	41.3	34.5	5. *J. Membr. Sci.* **538,** 9–17 (2017).
	PIP/H_2N-PEG-NH_2 2 kDa	5.8	99.5	58.3	83.4	
	PIP/H_2N-PEG-NH_2 (After NaClO treatment)	5.6	97.9	50.5	23.6	
Polypiperazine-amide NF membrane modified by different functionalized Multiwalled Carbon Nanotubes (MWCNTs)	MWCNT-COOH/ polyamide (PIP/TMC)	6.2	96.6	34.0	19.4	6. *ACS Appl. Mater. Interfaces.* **8,** 19135−19144 (2016).
	MWCNT-OH/ polyamide (PIP/TMC)	6.9	97.6	35.3	26.9	
	MWCNT-NH/ polyamide (PIP/TMC)	5.3	96.8	35.1	20.3	
NF membrane prepared from 1,4-	DCH – TMC	5.3	96.8	25.9	23.2	7. *RSC Adv.* **5,** 40742–40752 (2015).

diaminocyclohexane (DCH) and TMC	DCH/SCHS (0.07% w/v) – TMC	7.4	98.1	26.8	38.5	
Antifouling NF membranes prepared from fluorinated polyamine	FPA/TMC	6.4	51.2	23.2	1.6	8. *Ind. Eng. Chem. Res.* **54,** 8302−8310 (2015).
	TETA/TMC	NA	53.7	26.5	1.6	
pH resistant TFC polyamine NF membranes prepared from cyanuric chloride and monomeric amines	DETA/CC (6 bar)	[b]0.95	74.8	77.7	0.88	9. *J. Membr. Sci.* **523,** 487–496 (2017).
	DETA/CC (10 bar)	[b]1.3	77.6	85.2	0.66	
	DETA/CC (15 bar)	[b]1.3	78.3	85.6	0.66	
	DETA/CC (20 bar)	[b]1.4	79.6	83.1	0.83	
Nanofilms directly formed on macro-porous substrates	PDA/PEI/10 min	17.8	79.0	51.2	2.3	10. *J. Mater. Chem. A* **6,** 2908–2913 (2018).
Chlorine resistant NF membranes prepared from monomers of 1,2,4,5-benzene tetracarbonyl chloride and MPD	PAA-ion-EDA	[c]3.9	78.0	57.0	1.9	11. *J. Mater. Chem. A*. **3,** 8816–8824 (2015).
	PAA-cov-EDA	[c]3.2	83.0	30.0	4.1	
NF membrane prepared from cis, cis-1,3,5-triaminocyclohexane and TMC	TAC/TMC	1.6	98.2	54.6	25.2	12. *J. Appl. Polym. Sci.* **133,** 43511 (2016).
TFC membrane prepared from polyvinylamine and TMC for NF	PVAm – TMC (performance at pH 7)	8.5	94.8	59.6	7.8	13. *Desalination*. **288,** 98–107 (2012).
	PVAm – TMC (performance at pH 6)	NA	72.5	57.8	1.5	
Negatively charged polyimide NF membranes with high selectivity and performance stability	PI-NF after imidization	4.0	93.9	42.8	9.4	14. *J. Membr. Sci.* **563,** 752–761 (2018).
Acid stable TFC NF membrane prepared from naphthalene-1,3,6-trisulfonylchloride and piperazine	PIP-NTSC	5.8	86.8	50.5	3.7	15. *J. Membr. Sci.* **415–416,** 122–131 (2012).
Composite NF membranes prepared from tannic acid and TMC	Tannic acid/TMC-5#	23.4	47.0	15.0	1.6	16. *J. Membr. Sci.* **429,** 235–242 (2013).
A facial zwitterionization in the interfacial modification of low bio-fouling NF membranes	Virgin TMC/DETA	[b]4.5	60.0	32.0	1.7	17. *J. Membr. Sci.* **389,** 76–82 (2012).
	Q-IPA25	[b]4.7	52.0	45.0	1.1	
NF membrane prepared with polyhexamethylene guanidine hydrochloride and TMC	HDA-TMC/PSf	[b]2.8	79.1	39.9	2.8	18. *J. Membr. Sci.* **466,** 82–91 (2014).
	PHGH-TMC/PSf	[b]3.4	37.4	43.6	0.9	
Influence of hyperbranched polyester on	NF-G2	37.5	50.8	16.5	1.7	19. *J. Membr. Sci.* **440,** 67–76 (2013).

structure and properties of synthesized NF membranes	NF-G3	17.8	78.5	32.3	3.2	
	NF-G4	7.0	90.5	43.7	5.9	
Polyamide TFC NF membranes prepared from polyethyleneimine and its conjugates for the enhancement of selectivity and antifouling property	TFC_{PIP}	[b]8.0	92.0	37.0	7.9	20. *RSC Adv*. **6,** 4521–4530 (2016).
	$TFC_{PIP/PEI-1}$	[b]7.7	82.0	54.0	2.6	
	$TFC_{PIP/PEI–Dex-5}$	[b]8.6	91.0	36.0	7.1	
	$TFC_{PIP/PEI–PEG-5}$	[b]8.2	84.0	34.0	4.1	
pH-stable TFC membrane based on organic–inorganic hybrid composite materials for NF	PVA	1.7	88.6	NA	NA	21. *J. Membr. Sci.* **476,** 500–507 (2015).
	PVA-MPTES-0.6	0.58	97.2	NA	NA	
	PVA-SMPTES-0.6	2.2	98.0	50.6	24.7	
TFC NF membranes fabricated from polymeric amine, polyethylenimine embedded with monomeric amine, piperazine for enhanced salt separations	$PEI_{2.4}$-$PIP_{0.6}$/TMC	5.1	50.0	65.0	0.70	22. *Reactive & Functional Polymers* **86,** 168–183 (2015).
	$PEI_{0.6}$/TMC - $PIP_{2.4}$/TMC	1.2	68.0	78.0	0.69	
	$PEI_{0.6}$ -$PIP_{2.4}$/TMC	1.0	72.0	55.0	1.6	
	$PEI_{3.0}$/TMC	0.9	68.0	75.0	0.78	
	$PIP_{3.0}$/TMC	0.5	95.0	52.0	9.6	
NF membranes synthesized from hyperbranched polyethyleneimine	EDA/TMC	1.7	66.1	35.0	1.9	23. *J. Membr. Sci.* **326,** 19–26 (2009).
	DETA/TMC	4.5	59.2	34.0	1.6	
	PEI/TPC	3.1	74.2	61.0	1.5	
	PEI/TMC	9.5	51.0	45.0	1.1	
TFC reverse osmosis membranes and spiral wound modules	NS-300	5.5	98.0	50.0	25.0	24. *Desalination.* **51,** 79–92 (1984).
	NTR-7250	6.8	99.0	55.0	45.0	
Water and salt transport through polyamide composite membranes	NF 40-2514	[b]4.1	[a]93.8	42.1	9.3	25. *J. Membr. Sci.* **36**, 297–313 (1988).
NF membranes broaden the use of membrane separation technology	XP 45	4.8	[a]97.5	50.0	20.0	26. *Desalination*. **70,** 77–88 (1988).
	XP 20	3.4	[a]85.0	20.0	5.3	
	NF 70	8.5	[a]97.5	75.0	10.0	
Poly(piperazineamide) composite NF membranes from 3,3',5,5'-biphenyl tetraacyl chloride and piperazine	mm-BTEC/PIP	[c]10.3	95.0	65.0	7.0	27. *J. Membr. Sci.* **335,** 133–139 (2009).
	TMC/PIP	[c]7.0	97.5	NA	NA	
Polypiperazine amide/PPESK hollow fiber TFC NF membranes	PPESK PIP/TMC hollow fibre	15.4	99.0	26.8	73.2	28. *J. Membr. Sci.* **301,** 85–92 (2007).
NF membrane prepared with PAMAM and TMC by interfacial polymerization on PEK-C ultrafiltration support	NF2 G0 (4)	6.3	38.2	36.2	1.0	29. *J. Membr. Sci.* **269,** 84–93 (2006).
	NF5 G1 (8)	7.6	47.6	48.1	1.0	
	NF9 G2 (16)	11.4	58.2	72.5	0.66	

Polyelectrolyte complex/MWCNT hybrid NF membranes for water softening	PEC-NFM-1	[b]1.0	85.5	8.4	6.3	30. *J. Membr. Sci.* **492,** 412–421 (2015).
	PEC-NFM-2	[b]1.2	54.1	8.4	2.0	
Very low pressure driven TFC membranes	NF40HF	6.1	[a]95.0	40.0	12.0	31. *Desalination*. **62,** 183–191 (1987).
Composite nanofiltration membrane incorporated with attapulgite nanorods for high water flux and antifouling property	PA-ATP(5)/PES composite membrane	22.9	92.0	14.7	10.7	32. *J. Membr. Sci.* **544,** 79–87 (2017).
Enhancing the performance of polyethylenimine modified NF membranes by coating a layer of sulfonated poly(ether ether ketone) for removing sulfamerazine	SPEEK/PEI-PI # 0 m	3.9	15.8	33.2	0.8	33. *J. Membr. Sci.* **492,** 620–629 (2015).
	SPEEK/PEI-PI # 5 m	3.4	69.7	57.6	1.4	
	SPEEK/PEI-PI # 10 m	2.9	86.6	60.8	2.9	
	SPEEK/PEI-PI # 30 m	2.3	86.6	66.9	2.5	
	SPEEK/PEI-PI # 60 m	2.0	86.6	70.4	2.2	
A tight NF membranes with multi-charged nanofilms for high rejection to concentrated salts	M0	NA	98.0	15.0	42.5	34. *J. Membr. Sci.* **537,** 407–415 (2017).
	M2 (PDA/PEI)	NA	70.9	45.3	1.9	
	M3 (PDA/PEI/PAA)	5.5	98.3	59.0	24.1	
NF membranes based on nucleophilic nature of polydopamine	M-PDA	76.3	20.5	1.4	1.2	35. *J. Membr. Sci.* **511,** 65–75 (2016).
	M-TMC	11.4	72.5	18.4	3.0	
	M-PEI	3.5	44.0	64.1	0.6	
Fabrication and performance of a new type of charged NF membranes based on polyelectrolyte complex	PECNM1-2	[b]1.4	[*]87.7	24.2	6.2	36. *J. Membr. Sci.* **357,** 80–89 (2010).
	PECNM2	[b]1.9	[*]91.8	24.2	9.2	
	PECNM3	[b]1.2	[*]91.2	25.7	8.4	
NF using diethanolamine-modified polyamide TFC membranes	Traditional PA-TFC	13.4	98.6	51.5	34.6	37. *Sep. Purif. Technol.* **173,** 135–143 (2017).
	DEA-modified PA-TFC	17.0	98.5	50.6	32.9	
Polyester composite NF membranes by interfacial polymerization of triethanolamine and TMC	TEOA (5 % w/v)/TMC	0.82	54.9	28.1	1.6	38. *J. Membr. Sci.* **320,** 198–205 (2008).
	TEOA (6 % w/v)/TMC	0.52	82.2	42.2	3.2	
Incorporating hyperbranched polyester into crosslinked polyamide layer to enhance both permeability and selectivity of NF membranes	NF0	7.0	96.8	30.0	21.9	39. *J. Membr. Sci.* **518,** 141–149 (2016).
	NF3	9.4	98.8	32.5	56.2	
	NF6	11.4	99.0	30.5	69.5	
	NF8	15.4	95.9	21.2	19.2	
Mixed polyamide-based composite NF hollow fiber membranes with improved	PEI only @ hollow fiber	15.3	50.4	44.6	1.1	40. *J. Membr. Sci.* **468,** 52–61 (2014).
	PEI/PIP @ hollow fiber	18.2	77.4	53.6	2.1	

low-pressure water softening capability	PIP only @ hollow fiber	6.8	99.3	13.6	123	
	Dow-Filmtec NF90	6.7	[a]97.0	90.0	3.3	
	Dow-Filmtec NF270	13.2	98.0	51.0	24.5	
	Koch TFC-SR2	14.5	[a]92.0	20.0	8.0	
Selective separation of chloride and sulfate by nanofiltration for high saline wastewater recycling	Desal-DL membrane @ 4 g/L salt concentration	7.4	98.8	37.2	52.3	41. *Sep. Purif. Technol.* **166,** 135–141 (2016).
Study on the thin-film composite nanofiltration membrane for the removal of sulfate from concentrated salt aqueous: Preparation and performance	Type A @ 40 sec	7.8	[a]98.8	65.5	28.7	42. *J. Membr. Sci.* **310,** 289–295 (2008).
	Type B @ 80°C	7.7	[a]98.5	66.5	22.3	
	Type C @ 5 min	7.5	[a]99.0	68.0	32.0	
	Type D @ NaOH	4.8	[a]98.2	65.0	19.4	
	Type D @ NaH_2PO_4	7.6	[a]98.4	67.5	20.3	
	Desal-5	4.7	[a]96.0	50.0	12.5	
	NF-70	7.2	[a]98.0	70.0	15.0	
	NTR-7250	6.2	[a]98.0	50.0	25.0	
	UTC-60	4.7	[a]99.0	85.0	15.0	
Ion transport characteristics in NF membranes: measurements and mechanisms	GE-Osmonics HL	6.9	[a]97.0	33.0	22.3	43. *J. Water Supply: Research and Technology – AQUA* **59,** 179–190 (2010), 40. *J. Membr. Sci.* **468,** 52–61 (2014).
Effect of hydrophilic and hydrophobic organic matter on amoxicillin and cephalexin residuals rejection from water by nanofiltration	TFC-SR2	7.5	[a]92.0	24.0	9.5	44. *Iran. J. Environ. Health. Sci. Eng.* **7,** 15–24 (2010).
	TFC-SR3	2.1	[a]93.0	38.0	8.8	
High performance silica-fluoropolyamide NF membranes prepared by interfacial polymerization	Silica-fluoropolyamide	2.6	85.0	13.0	5.8	45. *Sep. Purif. Technol.* **110,** 31–38 (2013).
	Silica-fluoropolyamide treated with NaOCl	17.5	94.0	13.5	14.4	
pH-responsive NF membranes containing carboxybetaine with tunable ion selectivity for charge-based separations	PCHM1	2.2	83.4	5.2	5.7	46. *J. Membr. Sci.* **520,** 294–302 (2016).
	PCHM2	3.8	74.4	4.4	3.7	
	PCHM3	5.0	50.0	3.9	1.9	
	PCHM4	7.0	25.0	2.2	1.3	
Influence of ion size and charge in NF	Nitto-Denko NTR-7450	10.9	92.0	53.0	5.9	47. *Sep. Purif. Technol.* **14,** 155–162 (1998).
	Filmtec NF-40	NA	96.0	47.0	13.3	
Biocatalytic and salt selective multilayer polyelectrolyte NF membranes	(PEI-PSS)2	8.0	59.5	28.5	1.8	48. *J. Membr. Sci.* **549,** 357–365 (2018).
	(PDADMAC-PSS)2	19.0	85.1	38.0	4.2	

	(PDADMAC-PSS)4	14.0	94.2	45.5	9.4	
	(PDADMAC-PSS)6	13.0	94.2	35.7	11.1	
Effect of substrate on formation and NF performance of graphene oxide membranes	GO/PAN membrane	[b]16.2	70.0	30.5	2.3	49. *J. Membr. Sci.* **574,** 196–204 (2019).
Crosslinked layer-by-layer polyelectrolyte NF hollow fiber membranes for low-pressure water softening	LBL@2	[b]9.6	[a]93.0	58.6	5.9	50. *J. Membr. Sci.* **486,** 169–176 (2015).
	LBL@1.5C	[b]14.4	95.2	33.5	13.9	
	Dow Filmtec™ NF270	13.1	98.1	37.1	33.1	
	Dow Filmtec™ NF90	6.7	98.6	68.6	22.4	
High performance enzyme-triggered coatings of tea catechins/chitosan	Catechins/chitosan co-deposited TFC NFMs	7.5	98.9	39.5	55.0	51. *Green Chem.* **18,** 6205–6208 (2016).
Effect of amine spacer of PEG on the properties, performance and antifouling behavior of poly(piperazineamide) TFC NF membranes	$NF_{AA\text{-}PEG\text{-}AA(0.5\%)}$	7.4	93.0	46.0	7.7	52. *J. Membr. Sci.* **472,** 154–166 (2014).
	$NF_{MPD\text{-}PEG\text{-}MPD(0.5\%)}$	5.2	83.0	43.0	3.4	
	$NF_{H2N\text{-}PEG\text{-}NH2(0.5\%)}$	5.6	87.0	46.0	4.2	
The effect of phenol functionality on the performance of polyester thin film composite NF membranes	TFC5	[b]7.8	93.0	65.0	5.0	53. *RSC Adv.* **6,** 99867–999877 (2016).
	TFC6	[b]7.4	92.0	68.0	4.0	
In situ manipulation of properties and performance of polyethyleneimine NF membranes by polyethylenimine-dextran conjugate	$TFC_{PEI(0.25)}$	3.6	85.0	36.0	4.3	54. *J. Membr. Sci.* **519,** 64–76 (2016).
	$TFC_{Dex\text{-}PEI + PEI(2.75,0.25)}$	7.4	85.0	36.0	4.3	
	$TFC_{PEI\text{-}Dex + PEI(3,0)}$	15.4	69.0	10.0	2.9	
High-selectivity hollow fiber composite NF membranes by two-way coating technique	HFC NF membrane	[b]5.7	[a]98.1	18.6	42.8	55. *J. Appl. Polym. Sci.* **131,** 41187 (2014).
Thin film nanocomposite membranes enabled by modified hydrophilic MOFs for NF	TFC	[b]5.9	93.3	26.7	10.9	56. *ACS Appl. Mater. Interfaces*. **9,** 1975−1986 (2017).
	TFN-mZIF1	[b]12.1	93.6	17.8	12.8	
	TFN-mZIF2	[b]14.5	93.3	10.0	13.4	
	TFN-mZIF3	[b]10.7	89.2	10.0	8.3	
NF membranes with high salt selectivity and performance stability using polyelectrolyte multilayers	M_N	7.8	78.1	61.9	1.7	57. *Desalination* **351,** 19–26 (2014).
	M_0	11.6	47.9	10.4	1.7	
	$M_{0.5}$	5.3	70.7	30.0	2.4	
	$M_{1.0}$	4.4	74.0	30.0	2.7	
	$M_{1.5}$	2.9	73.9	22.5	3.0	

	$M_{2.0}$	7.2	50.4	21.1	1.6	
Bio-inspired fabrication of high perm-selectivity and anti-fouling membranes based on zwitterionic polyelectrolyte nanoparticles	TFC	[b]5.5	97.2	31.9	24.3	58. *J. Mater. Chem. A* **4,** 4224–4231 (2016).
	TFN-ZPNP1	[b]9.6	97.4	15.1	32.7	
	TFN-ZPNP2	[b]10.0	97.2	11.4	31.6	
	TFN-ZPNP3	[b]10.8	97.0	9.3	30.2	
TFC NF membranes	PRP/TMC	[b]2.3	[a]95.0	39.0	12.2	59. *J. Appl. Polym. Sci.* **95,** 1251–1261 (2005).
	PPD/TMC	[b]1.3	[a]99.0	75.0	25.0	
NF membranes prepared by interfacial polymerization with zwitterionic amine monomers	NFM-0	[b]4.2	[a]87.7	30.9	5.6	60. *J. Membr. Sci.* **431,** 171–179 (2013).
	NFM-1	[b]4.9	[a]91.4	29.4	8.2	
	NFM-2	[b]6.5	[a]89.7	26.7	7.1	
	NFM-3	[b]7.4	[a]89.9	25.9	7.3	
	NFM-4	[b]7.6	[a]90.0	25.9	7.4	
Polyamide TFC membranes covalently bonded with modified mesoporous silica nanoparticles	mMSN/PA TFN	5.4	80.2	29.7	3.6	61. *J. Membr. Sci.* **428,** 341–348 (2013).
Composite NF membranes incorporated SiO_2 nanoparticles	NF1(G0, 0.5% SiO_2)	2.4	81.2	43.4	3.0	62. *Polymer* **53,** 5295–5303 (2012).
	NF2(G0, 1.5% SiO_2)	1.5	92.6	46.0	7.3	
	NF3(G1, 0.5% SiO_2)	2.0	91.5	46.4	6.3	
	NF4(G1, 1.0% SiO_2)	2.4	96.4	50.2	13.8	
Fabrication of polyamide thin-film nano-composite membranes with hydrophilized ordered mesoporous carbon	H-OMCs 0 wt%	[b]0.65	93.9	68.4	5.2	63. *J. Membr. Sci.* **375,** 46–54 (2011).
	H-OMCs 1 wt%	[b]0.64	89.7	51.0	4.8	
	H-OMCs 6 wt%	[b]0.65	88.4	47.0	4.6	
Graphene oxide modified polyamide NF membranes with improved flux and antifouling properties	TFC	[b]0.18	95.1	89.0	2.2	64. *J. Mater. Chem. A* **3,** 2065–2071 (2015).
	TFN-GO-0.2wt%	[b]1.7	94.6	88.8	2.1	
	TFN-GO-0.3wt%	[b]1.5	93.9	88.8	1.8	
Composite reverse osmosis and NF membranes	NS-300	[b]5.2	97.8	50.0	22.7	65. *J. Membr. Sci.* **83**, 81–150 (1993).
	Piperazine (control)	[b]4.6	97.0	53.0	15.7	
	NTR-7450	9.2	92.0	51.0	6.1	
	Cellulose acetate	3.0	96.0	54.0	11.5	
	NF40	2.1	[a]95.0	45.0	11.0	
	NF50	10.7	[a]90.0	50.0	5.0	
	NF70	7.2	[a]98.0	70.0	15.0	

Improved antifouling properties of polyamide NF membranes by reducing the density of surface carboxyl groups	TMC membrane	6.2	[a]94.5	30.2	12.7	66. *Environ. Sci. Technol.* **46,** 13253−13261 (2012).
	IPC membrane	2.9	[a]77.7	51.8	2.2	
High-flux TFC NF membranes fabricated by the NaClO pre-oxidation of the mixed diamine monomers of PIP and BHTTM	PIP + BHTTM + NaClO + NaOH	26.8	92.1	37.1	8.0	67. *J. Membr. Sci.* **502,** 106–115 (2016).
Polyamide thin-film composite NF membranes modified with poly(amidoamine) and SiO_2 gel	PAMAM–NH_2 G4	3.4	87.2	39.6	4.7	68. *RSC Adv.* **6,** 45585–45594 (2016).
	PAMAM–NH_2 G5	3.1	92.3	40.9	7.7	
	PAMAM–NH_2/PIP	5.3	91.5	31.9	8.0	
	PAMAM(G4,G5) + PIP + SiO_2 gel	6.4	92.0	35.2	8.1	
NF membranes with cellulose nanocrystals as an interlayer for unprecedented performance	PA50/CNC/PES	[b]32.3	97.7	6.5	40.7	69. *J. Mater. Chem. A* **5,** 16289–16295 (2017).
Single-walled carbon nanotube film supported NF membranes	PD/SWCNTs	[b]40.2	95.9	22.7	18.9	70. *Small* **12,** 5034–5041 (2016).
TFC membranes combining carbon nanotube intermediate layer and microfiltration support for high NF performances	NFM-UF	7.6	97.9	40.6	28.3	71. *J. Membr. Sci.* **515,** 238–244 (2016).
	NFM-06	17.5	97.2	34.1	23.5	
	NFM-12	13.1	94.1	35.0	11.0	
	NFM-24	10.9	95.8	35.2	15.4	
	NFM-36	8.7	97.6	36.0	26.7	
A route for surface zwitterionic functionalization of polyamide NF membranes with improved performance	NFM-0	[b]5.4	99.5	46.4	107.2	72. *J. Membr. Sci.* **490,** 311–320 (2015).
	NFM-1	[b]7.8	99.5	43.4	113.2	
	NFM-2	[b]9.8	99.5	44.0	112.0	
	NFM-3	[b]9.3	99.5	43.0	114.0	
NF membranes with chlorine-tolerant property and good separation performance	m-XDA 100 (M1)	3.9	95.4	35.7	14.0	73. *RSC Adv.* **8,** 36430–36440 (2018).
	m-XDA 80 (M2)	4.2	97.5	43.8	22.5	
	m-XDA 60 (M3)	4.6	97.1	39.5	20.9	
	m-XDA 40 (M4)	5.2	97.5	39.5	24.2	
	m-XDA 20 (M5)	6.4	96.5	32.3	19.3	
	m-XDA 0 (M6)	8.9	96.0	30.2	17.5	
Composite NF membranes via the co-deposition and cross-linking of catechol/ polyethylenimine	CCh/PEI = 4:1, 4 h	[b]4.5	88.4	41.5	5.0	74. *RSC Adv.* **6,** 34096–34102 (2016).

Ultrathin polyamide membranes with decreased porosity designed for outstanding water-softening performance and superior antifouling properties	TMC−PIP	[b]6.3	98.8	46.5	44.5	75. *ACS Appl. Mater. Interfaces* **10,** 43057−43067 (2018).
	C-TMC−MPD	[c]7.8	99.2	97.5	3.1	
	BTC−PIP	[b]9.7	99.1	83.3	18.5	
Polyamide TFC NF membranes modified with acyl chlorided graphene oxide	No added material	1.9	95.1	35.5	13.2	76. *J. Membr. Sci.* **535,** 208–220 (2017).
	GO-COCl	4.7	86.9	23.3	5.9	
	GO-COCl	3.8	97.1	57.2	14.8	
Improving the water permeability and antifouling property of thin-film composite polyamide NF membranes by modifying the active layer with triethanolamine	NFM-0	14.2	98.4	52.0	30.0	77. *J. Membr. Sci.* **513,** 108–116 (2016).
	NFM-1	15.8	98.2	50.3	27.6	
	NFM-2	16.3	98.2	50.1	27.7	
	NFM-3	17.0	98.2	49.9	27.8	
	NFM-4	17.2	98.2	49.7	27.9	
Ionic complexing induced fabrication of highly permeable and selective polyacrylic acid complexed poly (arylene ether sulfone) NF membranes	PES-TA	2.7	11.6	19.4	0.9	78. *J. Membr. Sci.* **520,** 130–138 (2016).
	PES-TA-PAA	6.5	96.8	60.9	12.2	
Polypiperazine-amide TFC NF membranes containing silica nanoparticles	Silica Sol (0.0 % w/v)	7.8	97.4	22.8	29.7	79. *Desalination* **301,** 75–81 (2012).
	Silica Sol (0.01 % w/v)	7.4	96.8	22.3	24.3	
	Silica Sol (0.05 % w/v)	8.7	97.0	24.7	25.1	
	Silica Sol (0.1 % w/v)	9.5	97.3	25.5	27.6	
	Silica Sol (0.5 % w/v)	10.3	96.6	19.9	23.6	
	Silica Sol (1.0 % w/v)	11.3	91.4	9.1	10.6	
Separation membranes based on zwitterionic colloid particles: tunable selectivity and enhanced antifouling property	ZCPM3@pH 7	[b]4.1	87.6	4.7	7.7	80. *J. Mater. Chem. A* **1,** 12213–12220 (2013).
	ZCPM3@pH 9	[b]4.2	91.0	6.6	10.4	
	ZCPM3@pH 10	[b]4.2	92.6	7.3	12.5	
Development of a highly hydrophilic NF membranes for desalination and water treatment	Unmodified	9.7	95.0	66.6	6.7	81. *Desalination* **168,** 215–221 (2004).
	Modified	11.9	96.1	62.5	9.6	
Graphene oxide embedded polyamide NF membranes for selective ion separation	Without GO	14.5	92.6	34.9	8.8	82. *J. Mater. Chem. A* **5,** 25632–25640 (2017).
	With GO	18.2	91.2	31.6	7.8	
Oligo-ethylene-glycol based thin-film composite NF membranes for effective	PA@EDA 0.15%	4.2	98.0	24.8	37.6	83. *J. Mater. Chem. A* **7,** 1849–1860 (2019).
	PA@EDA 1%	1.1	91.2	27.6	8.2	

separation of mono-/di-valent anions	PA@EDA 2%	0.6	61.4	27.5	1.9	
	PA@DCA 0.2%	8.3	98.5	12.6	58.3	
	PA@DCA 1.5%	1.5	96.5	17.5	23.6	
	PA@DCA 2.5%	1.3	95.0	13.2	17.4	
High-flux graphene oxide NF membranes intercalated by carbon nanotubes	GNm	4.7	95.1	59.0	8.4	84. *ACS Appl. Mater. Interfaces* **7,** 8147−8155 (2015).
	G-CNTm (8:1)	8.0	80.9	51.4	2.5	
	G-CNTm (4:1)	8.0	81.0	44.8	2.9	
	G-CNTm (8:3)	9.5	83.5	48.1	3.1	
	G-CNTm (2:1)	11.3	81.0	39.7	3.2	
	G-CNTm (8:5)	12.1	71.2	39.6	2.1	
Graphene oxide NF membranes stabilized by cationic porphyrin for high salt rejection	GOLM-100−6/30	[c]1.2	87.7	29.0	5.8	85. *ACS Appl. Mater. Interfaces*. **8,** 12588−12593 (2016).
Enabling graphene oxide nanosheets as water separation membranes	PSf-PDA-GO-15L	27.6	88.0	59.0	3.4	86. *Environ. Sci. Technol.* **47,** 3715−3723 (2013).
Enhanced desalination performance of carboxyl functionalized graphene oxide NF membranes	GO-COOH@0.5g/m^2	2.4	91.3	48.2	6.0	87. *Desalination* **405,** 29–39 (2017).
	GO@0.5g/m^2	1.9	90.0	42.8	5.7	
Cation-dependent structural instability of graphene oxide membranes and its effect on membranes separation performance	GO membrane	2.4	79.5	45.2	2.7	88. *Desalination* **399,** 40–46 (2016).
Thin-film composite membranes formed by interfacial polymerization with natural material sericin and TMC	NF8	11.9	95.3	41.0	12.5	89. *J. Membr. Sci.* **471,** 381–391 (2014).
Thin-film composite NF membranes with improved acid stability prepared from naphthalene-1,3,6-trisulfonylchloride and TMC	M1-NTSC-0	5.5	98.2	63.5	20.3	90. *Desalination* **315,** 164–172 (2013).
	M4-NTSC-0.015	8.4	98.4	56.5	27.2	
	M6-NTSC-0.025	10.6	97.8	51.5	22.0	
Tailoring the structure of polyamide TFC membranes with zwitterions to achieve high water permeability and antifouling property	TFCM-1	3.5	92.4	38.1	8.1	91. *RSC Adv.* **5,** 98730–98739 (2015).
	TFCM-2	1.6	86.7	64.8	2.6	
	TFCM-3	13.3	78.1	14.3	3.9	

Poly(p-phenylene terephthamide) embedded in a polysulfone as the substrate for improving compaction resistance and adhesion of a TFC polyamide membranes	PA/PSf	5.9	98.8	66.3	28.1	92. *J. Mater. Chem. A* **5,** 13610–13624 (2017).
	PA-PPTA/PSf 8	8.5	99.1	63.6	40.4	
A poly(amide-co-ester) NF membranes using monomers of glucose and TMC	NF-2G	[c]8.3	94.5	54.9	8.2	93. *J. Membr. Sci.* **504,** 185–195 (2016).
Chlorine resistant TFN NF membranes incorporated with octadecylamine-grafted GO and fluorine-containing monomer	TFCPIP-0	[c]3.2	98.3	41.5	34.4	94. *J. Membr. Sci.* **545,** (2018) 185–195.
	TFCMA-0	[c]5.3	95.2	30.6	14.5	
	TFNMA-GO	[c]9.0	94.0	28.8	11.9	
	TFNMA-GO-ODA	[c]8.3	98.5	34.3	43.8	
Graphene oxide polypiperazine-amide NF membranes for improving flux and anti-fouling in water purification	PPA/GO-M0	[b]11.0	98.2	58.7	22.9	95. *RSC Adv.* **6,** 82174–82185 (2016).
	PPA/GO-M3	[b]14.6	99.2	56.8	54.0	
Reduced graphene oxide-NH_2 modified low pressure NF composite hollow fiber membranes with improved water flux and antifouling capabilities	R-GO-NH_2	19.3	98.5	26.9	48.7	96. *Appl. Surf. Sci.* **419,** 418–428 (2017).
TiO_2@graphene oxide incorporated antifouling NF membranes with elevated filtration performance	NFM-3 # 0.2 wt% TiO_2@GO	5.9	98.8	31.4	57.2	97. *J. Membr. Sci.* **533,** 279–288 (2017).
TiO_2 NF membranes prepared by molecular layer deposition	AAO-60TiO_2	[b]10.5	43.0	29.0	1.2	98. *J. Membr. Sci.* **510,** 72–78 (2016).
Influence of silica nanospheres on the separation performance of TFC poly(piperazine-amide) NF membranes	TFCN	[c]3.9	[a]87.5	49.8	4.0	99. *Appl. Surf. Sci.* **324,** 757–764 (2015).
	TFNN	[c]4.5	[a]94.8	43.2	10.9	
High-flux TFC membranes for NF mediated by a rapid co-deposition of polydopamine/piperazine	PIP/dopamine: 0	[b]17.5	69.7	15.0	2.8	100. *J. Membr. Sci.* **554,** 97–108 (2018).
	PIP/dopamine: 1.0	[b]13.5	94.8	21.0	15.2	
	PIP/dopamine: 2.5	[b]10.8	96.8	23.7	23.8	
Influence of the diamine structure on the NF performance, surface morphology and surface charge of the composite polyamide membranes	PIP	6.6	95.0	40.0	12.0	101. *J. Membr. Sci.* **279,** 266–275 (2006).
	DAP	8.8	89.0	21.0	7.2	
	EAP	3.1	92.0	31.0	8.6	

Fabrication of NF membranes via stepwise assembly of oligoamide on alumina supports: Effect of number of reaction cycles on membrane properties	4.5 cycle	1.1	94.2	67.1	5.7	102. *J. Membr. Sci.* **543,** 269–276 (2017).
	5 cycle	0.64	91.0	76.2	2.6	
TFC NF membranes using different surfactants in organic phase	CTAB (0.0 % w/v)	4.6	85.1	48.9	3.4	103. *J. Membr. Sci.* **343,** 219–228 (2009).
	CTAB (0.1 % w/v)	4.5	89.3	56.8	4.0	
	CTAB (0.25 % w/v)	5.3	85.5	52.8	3.3	
	CTAB (0.5 % w/v)	5.1	82.2	69.4	1.7	
	SDS (0.0 % w/v)	4.6	84.6	49.1	3.3	
	SDS (0.1 % w/v)	4.9	82.5	46.0	3.1	
	SDS (0.25 % w/v)	8.3	81.9	51.2	2.7	
	SDS (0.5 % w/v)	7.7	88.5	42.6	5.0	
	Triton X-100 (0.0 % w/v)	4.6	84.6	49.1	3.3	
	Triton X-100 (0.1 % w/v)	5.3	70.5	58.3	1.4	
	Triton X-100 (0.25 % w/v)	2.9	64.5	51.6	1.4	
	Triton X-100 (0.5 % w/v)	1.5	50.8	63.6	0.7	
Interfacial polymerization on PES hollow fiber membranes using mixed diamines	PIP and BHTTM	5.2	99.7	43.8	187	104. *Desalination* **394,** 176–184 (2016).
Thin-film nanocomposite membranes embedded with poly(methyl methacrylate) hydrophobic modified MWCNT	MWCNTs (0.0 wt%)	4.3	98.1	36.6	33.4	105. *J. Membr. Sci.* **442,** 18–26 (2013).
	MWCNTs (0.33 wt%)	4.8	98.4	38.1	38.7	
	MWCNTs (0.67 wt%)	7.0	99.0	44.1	55.9	
	MWCNTs (1.30 wt%)	5.8	98.5	40.8	39.5	
High-performance acid-stable polysulfonamide TFC membranes prepared via spinning-assisted multilayer interfacial polymerization	sMIP PES-PSA_5	3.7	99.82	85.5	80.6	106. *J. Mater. Sci.* **54,** 886–900 (2019).
Improvement in desalination performance of thin film nanocomposite NF membranes using amine-functionalized multiwalled carbon nanotube	No CNT	[b]4.8	94.0	27.4	12.1	107. *Desalination* **394,** 83–90 (2016).
	CNT 0.001	[b]6.2	80.0	21.0	4.0	
	CNT 0.002	[b]5.8	80.8	28.3	3.7	
	CNT 0.005	[b]5.2	96.0	36.6	15.9	
	CNT 0.01	[b]5.0	94.3	26.8	12.8	
High permeanceTFC NF membrane with a polyelectrolyte complex top layer containing graphene oxide nanosheets	PEC-GO_{100} composite	[c]8.9	62.1	38.6	1.6	108. *J. Membr. Sci.* **540,** 391–400 (2017).

Tailoring the polyester/polyamide backbone stiffness for the fabrication of high performance NF membranes	PIP	5.2	98.3	41.3	34.5	109. *J. Membr. Sci.* **541,** 483–491 (2017).
	PIP/BPF	13.4	96.6	55.7	13.0	
	BPF	2.8	78.4	36.4	2.9	
Covalent organic framework modified polyamide NF membranes with enhanced performance for desalination	PA-SNW-1/PES (1g/m^2 loading)	19.2	83.5	15.3	5.1	110. *J. Membr. Sci.* **523,** 273–281 (2017).
Preparation of nanocavity-contained TFC NF membranes with enhanced permeability and divalent to monovalent ion selectivity	TFC_0	6.8	91.1	25.0	8.4	111. *Desalination* **445,** 115–122 (2018).
	TFC_{50}	9.8	97.8	21.9	35.5	
	TFC_{90}	20.2	81.3	17.4	4.4	
Highly permeable composite NF membranes made with acyl chloride monomer with an anhydride group	NFM-0	6.7	97.3	48.3	19.1	112. *J. Membr. Sci.* **570–571,** 403–409 (2019).
	NFM-4	13.2	97.6	34.0	27.5	
	NFM-7	17.0	95.9	34.9	15.9	
Polyamide membranes with nanoscale Turing structures for water purification	TS-I	[b]13.3	99.1	51.2	54.2	113. *Science* **360,** 518–521 (2018).
	TS-II	[b]25.8	99.6	49.6	126.0	
Multifunctional amine enables the formation of polyamide nanofilm composite ultrafiltration and NF membranes with modulated charge and performance	PEI-0.03 wt%	48.0	74.0	15.1	3.3	114. *J. Mater. Chem. A* **6,** 20242–20253 (2018).
	PEI-0.05 wt%	24.0	85.0	25.0	5.0	
	PEI-0.1 wt%	[b]18.6	77.1	26.0	3.2	
Graphene oxide incorporated thin film nanocomposite NF membranes for enhanced salt removal performance	GO loading 0 wt%	[b]1.6	94.1	31.0	11.7	115. *Desalination* **387,** 14–24 (2016).
	GO loading 0.1 wt%	2.2	94.1	52.4	8.1	
	GO loading 0.3 wt%	2.4	95.2	59.5	8.4	
	GO loading 0.5 wt%	2.4	95.2	64.7	7.4	
Nanoparticle-templated NF membranes for ultrahigh performance desalination	PD/ZIF-8 mass loading of 4.3 μg cm^{-2}	[c]53.5	95.2	10.9	18.6	116. *Nat. Commun.* **9,** 2004 (2018).
Preparation of TFC NF membranes with improved structural stability through the mediation of polydopamine	PA/PD-PES	11.4	93.5	31.0	10.6	117. *J. Membr. Sci.* **476,** 10–19 (2015).
	PA/PES	14.6	83.4	16.9	5.0	
Rapid water transport through controllable, ultrathin polyamide nanofilms for high-performance NF	Freestanding polyamide	25.1	99.1	27.5	80.6	118. *J. Mater. Chem. A* **6,** 15701–15709 (2018).

Transport, structural, and interfacial properties of poly (vinyl alcohol)–polysulfone composite NF membranes	PVA-PSf composite	3.9	90.0	37.4	6.3	119. *J. Membr. Sci.* **353,** 169–176 (2010).
	Dow Filmtec™ NF270	11.6	94.0	51.0	16.7	
Nanovoid membranes embedded with hollow zwitterionic Nano capsules	TFNM with HZN_CS	[b]16.5	94.7	38.2	11.7	120. *Nano Lett.* **19,** 2953−2959 (2019).
	TFNM with ZN_PS	[b]14.5	92.3	36.8	8.2	
	Control TFC NF	[b]10.5	92.1	32.7	8.5	
TFC membranes incorporated with metal-organic frameworks	TFC	6.89	98.8	32.7	56.0	121. *Ind. Eng. Chem. Res.* **58,** 8772–8783 (2019).
	TFN-0.05	12.68	99.1	39.8	66.9	
	TFN-0.10	14.55	99.0	38.1	61.9	
	TFN-0.15	13.13	98.9	35.4	58.7	
Hydrophilic hollow nanocubes functionalized thin film nanocomposite membranes	TFC	[c]10.3	93.5	40.2	9.2	122. *ACS Appl. Mater. Interfaces* **11,** 5344−5352 (2019).
	TFN-4H	[c]19.4	95.2	47.4	10.9	
	TFN-4S	[b]13.4	93.5	41.2	9.0	
Ultrathin NF membranes with polydopamine-covalent organic framework interlayer	PA/PAN	11.96	97.4	17.8	31.6	123. *J. Membr. Sci.* **576,** 131–141 (2019).
	PA/PDA/PAN	16.39	97.2	14.6	30.5	
	PA/PDA-COF(3)/PAN	20.7	93.4	19.6	12.2	
Ultrathin polyamide NF membranes fabricated on brush-painted single-walled carbon nanotubes	SWCNT (3 cycles)	[b]44.2	96.5	13.4	24.7	124. *ACS Nano* **13,** 5278−5290 (2019).
MOFs positioned polyamide membranes with fishnet-like structure	TFC	14.5	99.0	35.4	64.6	125. *J. Mater. Chem. A* **7,** 16313–16322 (2019).
	TFN-AU1	18.0	98.4	30.2	43.6	
	TFN-AU2	21.3	98.2	25.6	41.3	
	TFN-AU3	26.8	97.7	22.6	33.6	
	TFN-AU4	30.8	97.5	21.5	31.4	
The role of an interlayer for the fabrication of highly selective and permeable thin-film composite NF membranes	TFC-2	21.0	98.5	18.8	54.1	126. *ACS Appl. Mater. Interfaces* **11,** 7349−7356 (2019).
Sulfonated and carboxylated bulky diamine-diol and piperazine based negative charged NF membranes	SDA 2%	6.2	86.0	54.0	3.3	127. *Sep. Purif. Technol.* **222,** 284–296 (2019).
	SDA/PIP	5.0	97.0	78.0	7.3	
	CDA 2%	5.3	91.0	73.0	3.0	
	CDA/PIP	4.2	87.0	47.0	4.1	
	PIP	3.0	89.0	51.0	4.5	

High performance polyamide composite nanofiltration membranes with gelatin interlayer	PA/GE20/PAN	33.7	98.1	14.3	45.1	128. *J. Membr. Sci.* **588,** 117192 (2019).
Polyvinyl alcohol-assisted high-flux thin film nanocomposite NF membranes incorporated with halloysite nanotubes	HNTs	34.5	97.8	12.3	39.8	129. *Environ. Sci.: Water Res. Technol.* **5,** 1412–1422 (2019).
Thin-film composite membranes with aqueous template-induced surface nanostructures for enhanced NF	TFC-R	21.3	99.4	43.5	94.2	130. *J. Membr. Sci.* **589,** 117244 (2019).
	TFC-T	5.7	98.5	48.3	34.5	
High-performance NF membranes for high salinity separation in the chlor-alkali process	H-TFC	13.0	99.2	56.2	54.8	131. *Ind. Eng. Chem. Res.* **58**, 12280−12290 (2019).
Tannic acid/Fe^{3+} nanoscaffold for interfacial polymerization: toward enhanced nanofiltration performance	TFC0	2.2	75.8	10.3	3.7	132. *Environ. Sci. Technol.* **52,** 9341−9349 (2018).
	TFCn	19.7	95.2	17.2	17.2	
	Dow Filmtec™ NF270	13.2	99.2	49.5	63.1	
	Dow Filmtec™ NF90	6.5	98.2	64.4	19.8	
Controllable interfacial polymerization for NF membrane performance improvement by the polyphenol interlayer	PEI/TA-Psf NF with interlayer	10.8	99.0	48.0	52.0	133. *ACS Omega* **4,** 13824–13833 (2019).
Fabrication of composite polyamide /Kevlar aramid nanofiber nanofiltration membranes with high permselectivity in water desalination	ANF-TFC	14.4	100**	80.3	**	134. *J. Membr. Sci.* **592,** 117396 (2019).
	PMIA-TFC	1.6	99.6	98.3	4.3	
	NF90	8.3	100**	87.6	**	
	NF270	15.2	96.1	25.9	19.0	
Surface modified polyamide nanofiltration membranes with high permeability and stability	PIP-TMC-QAEP	[b]18.5	97.8	16.1	38.1	135. *J. Membr. Sci.* **592,** 117386 (2019).
	PIP-TMC	[b]6.2	98.8	56.3	36.4	
Polyamide thin film nanocomposite membranes with improved separation properties for water/ wastewater treatment	$TFN_{cyclo\text{-}0.05}$	7.5	96.4	18.9	22.5	136. *J. Mater. Chem. A* **4,** 4134–4144 (2016).
	TFC (control)	5.4	86.0	25.3	5.3	
Fabrication of high flux nanofiltration membrane via hydrogen bonding based co-deposition of polydopamine with poly(vinyl alcohol)	$M_{10\text{-}c}$ membrane	12.3	92.3	20.2	10.4	137. *J. Membr. Sci.* **552,** 222–233 (2018).
	$M_{2\text{-}c}$ membrane	13.6	94.2	22.3	13.4	

Improved performance of polyamide TFC NF membrane by using polyethersulfone/polyaniline membrane as the substrate	PA/PES/PANI-0.2	15.7	[a]95.0	33.0	13.4	138. *J. Membr. Sci.* **493,** 263–274 (2015).
Tuning the functional groups of carbon quantum dots in thin film nanocomposite membranes for nanofiltration	PA-TFC	3.0	95.5	30.2	15.5	139. *J. Membr. Sci.* **564,** 394–403 (2018).
	TFN-SCQD	7.0	93.8	8.8	14.7	
	TFN-NCQD	5.2	91.7	30.5	8.4	
	TFN-CCQD	6.1	93.6	16.8	13.0	
Polyamide/PVC based composite hollow fiber NF membranes	PVC-NF2	7.0	[a]98.0	30.0	35.0	140. *J. Membr. Sci.* **505,** 231–240 (2016).
An acid resistant NF membrane prepared from a precursor of poly (s-triazine-amine)	TPT-TMC/PSf TFC	[b]9.3	98.6	40.5	42.5	141. *J. Membr. Sci.* **546,** 225–233 (2018).
	PIP-TMC/PSf TFC	[b]8.2	97.6	54.2	19.1	
Covalent organic framework modulated interfacial polymerization for ultrathin desalination membranes	PA/CLS(5)	53.5	94.3	27.3	12.7	142. *J. Mater. Chem. A* **7,** 25641–25649 (2019).
Hydrogel assisted interfacial polymerization for advanced nanofiltration membranes	PIP 0.0175 wt%	52.8	96.4	17.0	23.0	143. *J. Mater. Chem. A* **8,** 3238–3245 (2020).
	PIP 0.015 wt%	62.9	93.5	10.5	13.8	
A facile and scalable fabrication procedure for thin film composite membranes	PIP-0.8-60	22.0	99.0	23.4	76.6	144. *Environ. Sci. Technol.* **54,** 1946-1954 (2020).
	PIP-0.3-60	34.7	95.5	12.2	19.5	
Acid resistant polysulfonamide thin-film composite nanofiltration membrane by a sulfonated poly(ether ether ketone) interlayer	PSA-PSF	[b]0.78	91.7	59.4	4.8	145. *Sep. Purif. Technol.* **239,** 116528 (2020).
	PSA/SPEEK-PSF	[b]1.9	99.4	88.5	19.2	
	SPEEK-PSF	[b]4.6	94.8	64.5	6.8	
Interfacial polymerization of piperazine and trimesoyl chloride with hydrophilic interlayer	TFC-PDA/PEI	[b]15.0	97.5	42.5	23.0	146. *Membranes* **10,** 12 (2020).
	TFC-TA/PEI	[b]16.7	97.8	43.6	25.6	
	TFC-ZIF-8/PEI	[b]19.9	98.2	45.2	30.4	
	TFC-PEG	[b]15.5	97.4	52.8	18.1	
	TFC-PVP	[b]18.4	98.2	53.6	25.8	
	TFC-PVA	[b]24.6	98.4	54.2	28.6	
Polyamide membranes with net-like nanostructures induced by different charged MOFs for elevated	Control	4.5	98.1	27.3	38.2	147. *ACS Appl. Polym. Mater.* **2,** 585–593 (2020).
	M-U1-A	9.7	95.7	25.1	17.4	
	M-U4-O	7.9	99.6	31.7	170.7	

nanofiltration						
Improved performance of thin-film nanofiltration membranes fabricated with the intervention of surfactants	TFC-Control	4.9	97.2	40.5	21.2	148. *Desalination* **481,** 114352 (2020).
	TFC-SDS	7.5	92.3	47.0	6.9	
Microwave heating assisted preparation of high permselectivity polypiperazine-amide nanofiltration membrane	PA/M-50 (PIP 0.05 / TMC 0.05)	26.2	97.7	17.0	36.0	149. *J. Membr. Sci.* **596,** 117718 (2020).
Nanofiltration membranes with narrowed pore size distribution via pore wall modification	NFMs@SMPS 12h	[c]3.3	96.2	16.0	22.1	150. *Chem. Commun.* **52,** 8589–8592 (2016).
Ultra-permeable polyamide membranes with covalent organic framework nanofiber scaffolds layer	PES-COFs scaffold/PIP-TMC polyamide	31.1	95.0	11.9	17.6	151. *Chem. Sci.* **10,** 9077–9083 (2019).
Ultrathin alginate coatings as selective layers for nanofiltration membranes with high performance	TFC NFMs with alginate selective layers	13.1	97.6	12.7	36.4	152. *ChemSusChem* **10,** 2788–2795 (2017).
NF membrane by cucurbituril-based host–guest chemistry	NF-PIP/TMC	5.7	95.8	49.5	12.0	153. *AIChEJ.* **66,** e16879 (2019).
	NF-0.1%-CB-1	15.5	94.9	18.3	16.0	
Superior NF membranes with gradient crosslinked selective layer fabricated via controlled hydrolysis	PA@A	5.6	92.0	23.0	9.6	154. *J. Membr. Sci.* **604,** 118067 (2020).
	PA@W-7	9.4	98.5	43.0	38.0	
	PA@W-0	27.5	98.5	52.5	31.6	
	PA@W-14	26.5	98.4	28.3	44.8	
Salt-tuned fabrication of novel polyamide composite nanofiltration membranes with three-dimensional Turing structures for effective desalination	PA20/PAN TFNC	25.8	99.1	26.1	82	155. *J. Membr. Sci.* **607,** 118153 (2020).
Phosphonium modification leads to ultrapermeable antibacterial polyamide composite membranes with unreduced thickness	THPC-5	50.5	98.4	22.0	48.8	156. *Adv. Mater.* **32**, 2001383 (2020).
An ultrahighly permeable-selective nanofiltration membrane mediated by an in situ formed interlayer	PIP–CSP_6/TMC	45.2	99.3	25.7	106	157. *J. Mater. Chem. A* **8,** 5275–5283 (2020).
Fabrication of thin-film composite polyamide nanofiltration membrane	NFM-15	23.7	99.4	33.4	114	158. *Desalination* **488,** 114525 (2020).

based on polyphenol intermediate layer with enhanced desalination performance						
Polyamide nanofiltration membrane with highly uniform sub-nanometre pores for sub-1 Å precision separation	(PIP+SDS) / TMC	17.1	99.6	27.0	182	159. *Nat. Commun.,* **11***,* 2015 (2020).
Ultrafast Ion Sieving from Honeycomb-like Polyamide Membranes Formed Using Porous Protein Assemblies	PA-1/MCE	84.0	99.0	13.7	86.3	160. *Nano Lett.*, 20, 5821–5829 (2020).
Root-like Polyamide Membranes with Fast Water Transport for High-performance Nanofiltration	E-PPA	48.9	93.9	30.0	11.5	161. J. Mater. Chem. A, 2020,8, 25028-25034.
High-Performance Zwitterionic Nanofiltration Membranes Fabricated via Microwave-Assisted Grafting of Betaine	TFC-0.2	40.8	97.0	12.9	29.0	162. *ACS Appl. Mater. Interfaces*, 12, 35523–35531 (2020).
Graphene quantum dots engineered ultrathin loose polyamide nanofilms	ULPA-2	32.1	99.6	17.7	205.8	163. J. Mater. Chem. A, 2020, 8, 23930-23938.
Molecularly soldered COF for ultrafast precision sieving	pDA/TpPa(W/E)-COF	60.9	99.5	49.2	101.6	164. Sci. Adv. 2021; 7: eabe8706.
Ultraselective and highly permeable polyamide nanofilms for ionic and molecular nanofiltration	PIP-0.05%-SLS 0 mM/TMC 0.05%-5s-HPAN support	47.9	98.47	14.2	56.1	165. Adv. Funct. Mater. 2021, 31, 2007054. (Reference [1] in the main manuscript)
	PIP-0.05%-SLS 0 mM/TMC 0.1%-5s-HPAN support	57.1	98.32	15.3	50.4	
	PIP-0.05%-SLS 0 mM/TMC 0.15%-5s-HPAN support	59.6	91.77	8.9	11.0	
	PIP-0.1%-SLS 0 mM/TMC 0.05%-5s-HPAN support	30.6	98.30	18.6	47.9	
	PIP-0.1%-SLS 0 mM/TMC 0.1%-5s-HPAN support	37.6	98.94	16.2	79.1	
	PIP-0.1%-SLS 0 mM/TMC 0.15%-5s-HPAN support	30.6	97.37	17.1	31.5	
	PIP-1.0%-SLS 0 mM/TMC 0.05%-5s-HPAN support	24.7	99.59	26.7	178.8	

PIP-1.0%-SLS 0 mM/TMC 0.1%-5s-HPAN support	19.3	99.65	37.9	177.4
PIP-1.0%-SLS 0 mM/TMC 0.15%-5s-HPAN support	15.9	99.63	30.1	188.9
PIP-2.0%-SLS 0 mM/TMC 0.05%-5s-HPAN support	17.6	98.65	38.4	45.6
PIP-2.0%-SLS 0 mM/TMC 0.1%-5s-HPAN support	18.6	98.60	24.2	54.1
PIP-2.0%-SLS 0 mM/TMC 0.15%-5s-HPAN support	14.7	98.75	47.9	41.7
PIP-0.01%-SLS 1 mM/TMC 0.1%-5s-HPAN support	59.0	98.18	9.7	49.6
PIP-0.01%-SLS 1 mM/TMC 0.15%-5s-HPAN support	58.8	96.78	10.3	27.9
PIP-0.05%-SLS 1 mM/TMC 0.05%-5s-HPAN support	22.6	99.92	41.1	736.3
PIP-0.05%-SLS 0.5mM/TMC 0.1%-5s-HPAN support	25.5	99.87	39.7	463.8
PIP-0.05%-SLS 1 mM/TMC 0.1%-5s-HPAN support	23.1	99.95	45.0	1100
PIP-0.05%-SLS 1 mM/TMC 0.15%-5s-HPAN support	22.2	99.95	40.1	1198
PIP-0.1%-SLS 1 mM/TMC 0.05%-5s-HPAN support	14.2	99.81	43.7	296.3
PIP-0.1%-SLS 1 mM/TMC 0.1%-5s-HPAN support	16.4	99.96	42.1	1447
PIP-0.1%-SLS 1 mM/TMC 0.1%-30s-HPAN support	15.1	99.98	42.9	2855
PIP-0.1%-SLS 1 mM/TMC 0.1%-2min-HPAN support	11.9	99.98	51.0	2448

PIP-0.1%-SLS 1mM/TMC 0.1%-20min-HPAN support	8.1	99.99	56.9	4310
PIP-0.1%-SLS 1 mM/TMC 0.1%-5s-PAN support	14.1	99.70	42.8	190.7
PIP-0.1%-SLS 1 mM/TMC 0.1%-5s-P84 support	45.6	90.65	11.3	9.5
PIP-0.1%-SLS 1 mM/TMC 0.1%-5s-PES support	24.9	98.53	20.4	54.1
PIP-0.1%-SLS 1 mM/TMC 0.1%-5s-HPAN support (heptane as organic phase)	13.3	99.78	41.5	265.9
PIP-0.1%-SLS 1 mM/TMC 0.1%-5s-HPAN support (cyclohexane as organic phase)	13.8	99.79	43.8	267.6
PIP-0.1%-SLS 1 mM/TMC 0.15%-5s-HPAN support	16.2	99.91	44.6	615.5

[#]PWP: Pure water permeance ($Lm^{-2}h^{-1}bar^{-1}$). [a]Rejection of $MgSO_4$. [b]Water permeance with NaCl feed was considered as pure water permeance. [c]Water permeance with $MgSO_4/Na_2SO_4$ feed was considered as pure water permeance. *Rejection of K_2SO_4. MPD: *m*-phenylenediamine, TMC: Trimesoyl chloride. Some data were read directly from the figures as there was no actual value given in the article and may have an error (no more than 0.5% of the full-scale data given in the figure) in reading the data from the figures. **not determined.